

GRANZYME B: ROLE IN SPINAL CORD INJURY AND IMPEDED REPAIR

by

Cameron Paul Oram

B.Sc., McGill University, 2013

A THESIS SUBMITTED IN PARTIAL FULFILLMENT OF
THE REQUIREMENTS FOR THE DEGREE OF

MASTER OF SCIENCE

in

THE FACULTY OF GRADUATE AND POSTDOCTORAL STUDIES
(Pathology and Laboratory Medicine)

THE UNIVERSITY OF BRITISH COLUMBIA
(Vancouver)

October 2018

© Cameron Paul Oram, 2018

The following individuals certify that they have read, and recommend to the Faculty of Graduate and Postdoctoral Studies for acceptance, a thesis/dissertation entitled:

Granzyme B: Role in spinal cord injury and impeded repair

submitted by Cameron Paul Oram in partial fulfillment of the requirements for
the degree of Master of Science
in Pathology and Laboratory Medicine

Examining Committee:

David Granville, Pathology and Laboratory Medicine

Supervisor

Catherine Pallen, Pathology and Laboratory Medicine

Supervisory Committee Member

Cornelia Laule, Pathology and Laboratory Medicine

Additional Examiner

Matthew Ramer, Zoology

Additional Examiner

Additional Supervisory Committee Members:

Wolfram Tetzlaff, Zoology

Supervisory Committee Member

Decheng Yang, Pathology and Laboratory Medicine

Supervisory Committee Member

Abstract

The inflammatory cascade following spinal cord injury (SCI) involves multiple cellular and molecular responses that can both aid and impede recovery. A large component of the wound response is the infiltration of immune cells that secrete pro-inflammatory cytokines and proteases. Granzyme B (GzmB) is a serine protease released by immune cells that negatively affects wound healing through its intracellular and extracellular protease activity. GzmB is abundant in neuroinflammatory conditions and contributes to neuron and oligodendrocyte cell death. In this study we investigate the role of GzmB in tissue injury, inflammation and functional recovery following SCI. An SCI was induced in wild-type (WT) and GzmB knockout (GzmB-KO) mice at thoracic level 9. Mouse locomotion was observed over the course of 6 weeks using three behaviour tests (Basso mouse scale, rotarod and horizontal ladder). Lesions were harvested for histological analysis and sections stained with markers for neurons (NeuN) and dyed for myelin (Eriochrome Cyanine). A second cohort of mice were maintained for 1 week after SCI and probed for GzmB expression and cellular localization. GzmB expression was probed using markers for macrophages or microglia (CD68). GzmB-KO mice exhibited significantly improved motor scores, increased myelin and neural survival compared to WT controls. GzmB expression was observed in macrophages at 7 days post injury. In summary, GzmB is elevated and contributes to neurotoxicity, demyelination and impaired functional recovery following SCI.

Lay Summary

Traumatic injury to the spinal cord can cause long-term paralysis and loss of control to different organs in the body including the bladder, digestive system and cardiovascular system. In spinal cord injuries, the immune system, the cells that protect your body from bacterial or viral infections, acts as a double-edged sword. While required to promote repair, too much inflammation can amplify the damage to the spinal cord and prevent recovery. As such, identifying molecules that are released from immune cells that cause damage and impede repair is an area of active investigation. My research identified Granzyme B as an immune-cell factor that contributes to spinal cord injury. We found that genetically removing Granzyme B reduces the amount of spinal cord injury and helps repair. This suggests that stopping Granzyme B after spinal cord injury may prevent further damage to the spinal cord and may help recovery.

Preface

- All *in vivo* experiments and behavioral analysis was performed by Cameron Oram with the assistance of Keir Martyn, under the supervision of Dr. David Granville.
- Blinded histological analysis was performed by Cameron Oram and Stephanie Santacruz.
- Experimental design was completed by Cameron Oram under the consultation of Dr. David Granville.
- The animal model used was done in collaboration with the lab of Dr. Wolfram Tetzlaff. Specifically, Dr. Jie Liu performed all murine spinal cord contusions.

Table of Contents

Abstract.....	iii
Lay Summary	iv
Preface.....	v
Table of Contents	vi
List of Tables	ix
List of Figures.....	x
List of Acronyms and Abbreviations	xi
Acknowledgements	xiii
Dedication	xiv
Chapter 1: Introduction	1
1.1 Spinal Cord Injury.....	1
1.2 Spinal Cord Biology	1
1.2.1 The Blood-Brain Barrier and Immune Surveillance	5
1.2.2 SCI Pathology	6
1.2.3 Inflammatory Response to SCI.....	7
1.2.4 Neurotoxicity and Demyelination.....	10
1.2.5 Glial and Fibrotic Scar	11
1.3 Granzymes	13
1.4 Granzyme Expression	14
1.5 Granzyme B Mediated Apoptosis.....	15
1.6 Extracellular Granzyme B.....	19
1.7 Granzyme B in Pathology	22

1.8	Granzyme B in Neuroinflammation.....	23
1.9	Rationale and Hypothesis	26
Chapter 2: Materials and Methods		28
2.1	Mice	28
2.2	Spinal Cord Contusion Injury	28
2.3	Mouse Behavioral Tests.....	29
2.3.1	Basso Mouse Scale	29
2.3.2	Rotarod.....	30
2.3.3	Horizontal Ladder Test	30
2.4	Animal Sacrifice and Tissue Processing.....	33
2.5	Eriochrome Cyanine Myelin Staining	33
2.6	Immunohistochemistry	34
2.7	RNA Extraction and qPCR.....	36
2.8	GzmB KO Genotyping	38
2.9	Image Analysis.....	38
2.10	Statistical Analysis.....	38
Chapter 3: Results.....		40
3.1	Spinal Cord Injury Parameters and Survival	40
3.2	Locomotive Recovery is Improved in GzmB KO Mice	42
3.3	Expression of GzmB in Mouse SCI.....	44
3.4	Preservation of White Matter in GzmB KO Mice Following SCI.....	46
3.5	Increased Neuron Survival Across SCI Lesion in GzmB KO Mice	46
3.6	Lack of GzmB Does not Influence Pro-Inflammatory Cytokine Expression	48

Chapter 4: Discussion	50
Chapter 5: Conclusions and Future Directions.....	55
Bibliography	58

List of Tables

Table 1 List of Antibodies and Reagents	35
Table 2 List of Primers Used for Genotyping and qPCR	37

List of Figures

Figure 1 Anatomical Layout of the Human Spinal Cord.....	3
Figure 2 Mechanism of Gzmb-Mediated Apoptosis.....	18
Figure 3 Consequences of Extracellular GzmB Activity.....	21
Figure 4 Mouse SCI Study Timeline..	32
Figure 5 Injury Parameters.....	41
Figure 6 Locomotive Function After SCI is Improved in GzmB KO Mice..	43
Figure 7 GzmB Expression in Mouse SCI Lesions.	45
Figure 8 White Matter Myelin and Neuron Survival is Increased in GzmB KO Mice	47
Figure 9 IL-1 β and TNF- α mRNA Expression in GzmB KO and WT Mice Post-SCI.....	49
Figure 10 Summary of Findings and Hypothesized Mechanism.....	57

List of Acronyms and Abbreviations

AAA	Abdominal aortic aneurysm
ALS	Amyotrophic lateral sclerosis
BBB	Blood brain barrier
BMS	Basso mouse scale
BSCB	Blood-spinal cord barrier
ChABC	Chondroitinase ABC
CNS	Central nervous system
CSF	Cerebrospinal fluid
CSPG	Chondroitin sulfate proteoglycan
CST	Cortico-spinal tract
CTL	Cytotoxic T-lymphocyte
EAE	Experimental autoimmune encephalomyelitis
EC	Eriochrome cyanine-R
ECM	Extracellular matrix
GFAP	Glial fibrillary acid protein
GZMA	Granzyme A
GZMB	Granzyme B
GZMB KO	Granzyme B knockout
GZMH	Granzyme H
GZMK	Granzyme K
GZMM	Granzyme M
MBP	Myelin basic protein

M-CSF	Macrophage colony stimulating factor
MMP	Matrix metalloproteinase
MOMP	Mitochondrial outer membrane permeability
MS	Multiple sclerosis
NK	Natural killer
NOS	Nitric oxide species
OCT	Optimal cutting temperature
OPC	Oligodendrocyte precursor cell
PAR-1	Protease activated receptor-1
PBS	Phosphate buffered saline
PNS	Peripheral nervous system
ProGZM	Pro-granzyme
ROS	Reactive oxygen species
SCI	Spinal cord injury
SLE	Systemic lupus erythmatosis
TBI	Traumatic brain injury
tSCI	Traumatic spinal cord injury
UVA	Ultraviolet A
VEGF	Vascular endothelial growth factor
WT	Wild-type

Acknowledgements

First and foremost I offer my thanks to my supervisor, Dr. David Granville, for his support and insight throughout my Masters. I would also like to thank the entire Granville Lab for their guidance and support. I had the privilege of working with many talented post-doctoral fellows who trained me in various experimental techniques including Dr.'s Matt Zeglinski, Chris Turner, Valerio Russo, Steve Shen, Sho Hiroyasu. Special thanks to my fellow graduate students who provided data analysis and emotional support including Keir Martyn, Stephanie Santacruz, Anna Wilhelm and Dr. Keerit Tauh. I would also like to acknowledge the assistance of members of the Tetzlaff lab and Ramer lab, particularly Dr. Gregory Duncan, Sohrab Manesh, Nicole Janzen and Seth Holland who assisted me in the surgical and behavioural protocols and assisted with the immunofluorescent experiments. Dr. Jie Liu performed all surgeries and without his help this project would never have happened.

I would like to thank ICORD for the seed grant that provided the funding to complete this project. Finally, I extend many thanks to the members of my graduate committee, Dr. Wolfram Tetzlaff, Dr. Catherine Pallen and Dr. Decheng Yang for their insight and encouragement.

Dedication

I dedicate this thesis to my parents, Kathy and Duncan, and my partner, Ken, for supporting me throughout my education.

Chapter 1: Introduction

1.1 Spinal Cord Injury

Spinal cord injuries (SCIs) are characterized by damage to the spinal cord resulting in neurological impairment of motor, sensory and autonomic functions below the level of injury. Injuries can be complete, in which the individual has a complete loss of mobility and sensation below the injury, or incomplete, in which partial sensory or motor function remains in select regions below the injury¹. SCI can be caused by direct physical trauma, such as car crashes, or non-physical traumas such as cancerous tumours, infection or the age-related condition cervical spondylotic myelopathy. In Canada an estimated 1400 individuals suffer new traumatic SCI (tSCI) each year, costing the health care system over \$2.5 billion in initial hospitalization annually^{2,3}. Moreover the lifetime economic burden of tSCI ranges from \$1.5 to \$3.0 million per individual depending on the severity of the injury³.

The functional deficits that arise due to SCI are due to disruption of the ascending and descending white matter tracts as well as the death of neurons within the gray matter. The presentation of these symptoms depends on the injury location with a loss of sensory or motor function to organs and muscles innervated by axons below the level of injury¹. SCI may also result in disruption of autonomic control of cardiovascular, urinary, gastrointestinal, respiratory, and sexual function^{4,5}. Furthermore, control of the immune system of individuals with SCI may be impaired due to faulty nervous and endocrine control, leading systemically to both immune impairment and chronic inflammation⁶.

1.2 Spinal Cord Biology

The spinal cord is a column of nerve tissue within the central nervous system (CNS) responsible for controlling motor and autonomic function and receiving sensory input from

the body. The human spinal cord is approximately 45 cm in length and is housed within the vertebral canal. The cord is divided into 30 unique segments along its length: 8 cervical, 12 thoracic, 5 lumbar and 5 sacral segments^{7,8}. Each segment contains a pair of dorsal and ventral roots that join in the intervertebral foramina to form a spinal nerve. The dorsal and ventral roots relay the afferent (sensory) and efferent (motor) information between the CNS and the peripheral nervous system (PNS). The spinal cord is surrounded by three membranes separating the cord from each vertebrae: the dura matter (closest to the vertebral column), arachnoid and pia matter (closest to spinal column).

The outer section of the spinal column contains white matter comprised of myelinated axonal tracts relaying information between the brain and body (Figure 1A)⁹. Oligodendrocytes also occupy the white matter and provide the lipid-rich myelin that wraps the axon. The white matter is anatomically subdivided into three regions, the anterior, lateral and posterior funiculi on either side of the spinal cord^{8,9}. The white matter is further subdivided into the ascending, descending and propriospinal tracts. Descending tracts transmit information from the brain to the spinal cord and include the corticospinal tract (CST), rubrospinal tract, vestibulospinal tract, tectospinal tract, interstitiospinal tract and the solitariospinal tract⁷. The CST is the largest descending tract, arising from the cerebral cortex⁸. 90% of the CST decussates (crosses over) at the lower medulla to form the lateral CST within the lateral funiculi while the remaining 10% form the anterior CST of the anterior funiculi that only decussates to the contralateral side at their terminal spinal level⁸. These fibers innervate primarily the ipsilateral motor neurons that control body and limb movements.

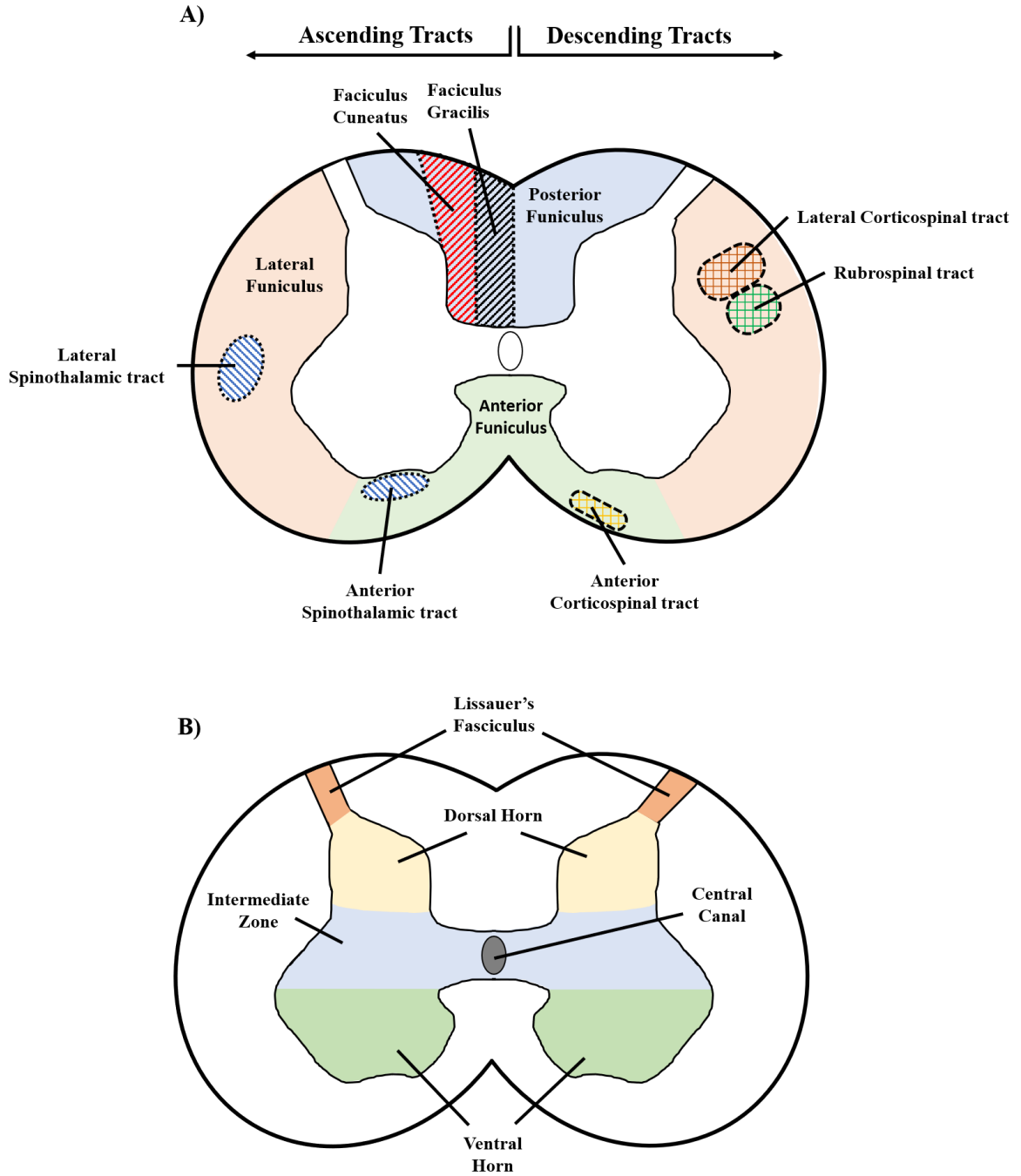


Figure 1: Anatomical Layout of the Human Spinal Cord. Layout of the different regions of the white matter (A) and gray matter (B) of the human spinal cord. Ascending and descending tracts appear on both sides of the white matter in (A).

The ascending tracts convey sensory information from the body to the brain. Two of the major sensory tracts are the dorsal column system, which transmit touch and proprioceptive information, and the spinothalamic tract, which conveys pain and temperature information⁹. The sensory tracts are composed of three successively connected neurons (first, second and third order neurons)⁷. The dorsal column system begins with first order neurons that carry sensory information from the legs and lower body through the medial fasciculus gracilis and sensory information from the arms and upper body through the more lateral fasciculus cuneatus⁷. These axons synapse with the second order neurons located in the nucleus gracilis or nucleus cuneatus of the medulla, which decussates the medulla midline and synapses with the third order neurons of the thalamus. The third order neurons travel into the cerebral cortex where sensory information is processed⁷. Spinothalamic tracts begin with sensory neurons with cell bodies in the dorsal root ganglia (first order neurons) that synapse with neurons in the dorsal horn. The second order neuron decussates above the level of entry and transmits information up spinal column tracts in the lateral or anterior region of the white matter. This second order neuron travels through the brainstem and synapses with the third order neuron located in the ventral posterolateral nuclei of the thalamus. The final neuron of the tract synapse within the cerebral cortex⁷.

While the outer white matter contains mostly myelinated axons with few cell bodies, the inner gray matter contains large numbers of neural cells bodies, oligodendrocytes and astrocytes. The inner gray matter contains symmetrical halves of neural tissue containing three major divisions: the dorsal (or posterior) horn, the intermediate zone and the ventral (or anterior) horn⁸ (Figure 1b). Dorsal horn neurons largely convey sensory information from the periphery, ventral horn neurons carry motor information out of the spinal cord while

intermediate zone neurons carry information related to autonomic functions. In addition to the motor and sensory neurons, gray matter also contain a network of interneurons that process sensory information, alter motor function and facilitate interlimb coordination through propriospinal neurons^{7,10,11}.

Cerebrospinal fluid (CSF) is contained within brain ventricles, the central canal of the spinal cord and the subarachnoid space (separating the arachnoid and pia matter of the meninges)¹². CSF plays a role in protecting the CNS from mechanical forces and maintaining homeostasis of neural cells¹³. CSF is secreted mainly by the choroid plexus of the brain and the ependymal cells that line the ventricles of the brain.

1.2.1 The Blood-Brain Barrier and Immune Surveillance

Blood supply is crucial to maintain the high metabolic demands of the CNS. A specialized blood-vessel structure termed the blood-brain barrier (BBB) and blood-spinal cord barrier (BSCB) regulates the passage of molecules between the blood and CNS¹⁴. The BBB is composed of endothelial cells in the subarachnoid space and pericytes and astrocytes located in the CNS parenchyma. Astrocytes are in direct contact with the neural circuitry within the CNS and can directly regulate cerebral blood flow depending on neuron activity¹⁵. The BBB includes two distinct basement membrane structures **i)** an inner vascular basement membrane, and **ii)** an outer parenchymal basement membrane composed of multiple extracellular matrix (ECM) proteins including type IV collagen, laminin, fibronectin and other glycoproteins¹⁶. The BBB can be altered in many neurological conditions, through damage to endothelial cells or the secretion of proteases such as matrix metalloproteinases (MMPs) that can degrade tight junction or basement membrane proteins¹⁷.

The tight junctions formed by the BBB prevents peripheral immune cells from entering the parenchyma of the CNS. BBB endothelial cells express low levels of leukocyte adhesion molecules such as selectins and ICAM-1 under healthy conditions, which reduces immune trafficking to the CNS¹⁸. Under neuroinflammatory conditions, such as in stroke or multiple sclerosis, there is an increase in immune cell infiltration into the brain parenchyma, mediated by an increase in chemokines and adhesion molecules from brain endothelial cells and the epithelial cells of the choroid plexus¹⁹⁻²².

Despite the restriction to peripheral immune cell infiltration, the CNS maintains a robust ability to respond to pathogens. Resident microglia cells survey the CNS in their quiescent form and can secrete cytokines and chemokines that increases BBB permeability and induces inflammation²³. In addition, there is a large population of immune cells (macrophages, mast cells, B-cells and T-Cells) located in the meninges that directly protect the CNS against pathogens²⁴. Finally, the CSF is connected to a lymphatic system that drains cellular and soluble antigens towards the cervical lymph nodes^{25,26}. It is theorized that CNS antigens are presented to immune cells that can direct immune cells response towards the brain or spinal cord.

1.2.2 SCI Pathology

The biological response to SCI is broken up into three temporal phases: Acute (seconds to minutes after injury), sub-acute (minutes to weeks) and chronic (months to years)²⁷. Tissue damage throughout this timeline is mediated by two mechanisms: primary injury and secondary injury²⁷. Primary injury encompasses the initial tissue damage associated with SCI. There are four distinct classes of primary injury: Impact with persistent compression, impact alone with transient compression, distraction, and laceration or

transection²⁷. SCI typically involves retropulsed vertebral fragments that apply compression or lacerate partially or fully through the spinal column²⁷. Primary injury leads to immediate and delayed resident cell death and disruption of the vasculature that leads to hemorrhage and/or ischemia in key functional regions of the spinal cord. In general, hemorrhage tends to primarily damage the central gray matter due to its high vascular content and its relatively soft tissue consistency²⁸. Grey matter is highly vascularized because of the large metabolic requirements of gray matter neurons²⁸.

Secondary injury encompasses the inflammatory response, and glial and vascular changes that accompany the primary trauma, evoking further tissue damage and limiting restorative capabilities²⁹. There are many mediators of secondary injury reported in the literature, including hemorrhage and ischemia-reperfusion, glutamatergic excitotoxicity, local inflammation, immune cell infiltration and cytokine secretion, necrotic or apoptotic neural cell death and the development of inhibitory glial and fibrotic scars³⁰⁻³⁴. These secondary injury cascades begin within minutes of the initial trauma and can last for weeks or months after the injury²⁹. For the purpose of this thesis, only the immune/inflammatory and glial/fibrotic scarring components of the secondary injury cascade will be discussed in full.

1.2.3 Inflammatory Response to SCI

The inflammatory response following SCI is composed of various cellular and molecular responses starting immediately after injury and continuing for several weeks or months³⁴⁻³⁷. Both resident glial and peripheral immune cells are involved in this injury response, characterized by activation and proliferation of resident cells (microgliosis, astrogliosis) and the secretion of proteases, cytokines and chemokines.

Traumatic SCI results immediately in breakdown of the BBB largely due to the mechanical disruption of capillary beds^{38,39}. This disruption makes the SCI lesion susceptible to infiltration by immune cells and neurotoxic blood proteins. While the BBB is capable of partially repairing itself, studies have reported that the barrier may remain compromised up to 56 days post injury in rats⁴⁰. Furthermore, locomotive recovery in rats was inversely correlated with BBB permeability levels, highlighting the importance of regenerating a functioning barrier between the blood and spinal cord. Proteases associated with SCI have been shown to alter the permeability of the BBB including MMP-3, MMP-9 and MMP-12⁴¹⁻⁴³.

Neutrophils are the first peripheral immune cell to infiltrate into an SCI lesion, peaking in number by 24 hours post injury and secreting proteases, cytokines and generating reactive oxygen species (ROS) that exacerbate a harmful tissue environment^{37,44}. Neutrophils are attracted to the CNS by the secretion of chemokines CXCL1, 2 and CCL3 by astrocytes⁴⁵. While little research has been conducted on the specific activities of neutrophil derived factors in SCI, *in vitro* studies have shown neutrophil derived MMP-9, ROS and tumor necrosis factor- α (TNF- α) are cytotoxic to dorsal root ganglion, a cluster of peripheral sensory neurons^{44,46}. Furthermore, reducing the number of infiltrating neutrophils into SCI lesions by inhibiting the LTB₄-BLT1 pathway attenuates secondary injury⁴⁷. Neutrophils typically clear within the lesion during the first week following injury in humans but can remain elevated in mice for months⁴⁵.

The resident microglial response occurs immediately following injury and is characterized by marked proliferation and migration to the lesion core^{48,49}. Resting, quiescent microglia take on a ramified morphology that changes to a rounded shape once activated.

Activated microglia can be seen within 12 hours post injury which typically peaks in numbers between 3-7 days post injury. Major factors secreted by microglia include the pro-inflammatory cytokines TNF- α , IL-1 β , IL-6, IL-12, NOS and macrophage colony stimulating factor (M-CSF) that largely function to recruit immune cell infiltration into the spinal cord^{50,51}. Peripheral monocytes begin migrating into the lesion 3 days post-injury and polarize into macrophages that become phenotypically and morphologically similar to activated microglia (rounded and CD68⁺/Iba-1⁺)⁵¹. These macrophages adopt classical M1 and alternatively-activated M2a expression of IL-6, TNF- α , IL-1 β and IL-12 for M1 and Arg, IL-4, CD206 and Fizz-1 for M2a⁵². Macrophages in normal wounds transition from M1 and M2a phenotypes to inflammation resolving and tissue remodeling M2b and M2c phenotypes⁵³. M2b macrophages secrete IL-10, an anti-inflammatory cytokine shown to prevent neural apoptosis in SCI⁵⁴. M1 macrophages can remain elevated at ~45% of their peak cellular number months after SCI, while M2 responses begin to decline after 7 days post-injury, highlighting the SCI microenvironment as a chronic non-resolving wound⁵².

Microglia/macrophages provide both regenerative and neurotoxic functions in the SCI lesion^{52,55-57}. In addition to killing pathogens that penetrate the BBB, microglia and macrophages can phagocytose tissue debris such as apoptosed neurons^{58,59}. In general, macrophage/microglia expressing M1 phenotypes secrete neurotoxic factors and altering their polarization towards the M2 phenotype reduces tissue damage (preservation of neurons, increased axon myelination) post SCI^{55-57,60}.

Lymphocyte infiltration into the injured spinal cord occurs within the first week and remains elevated thereafter⁶¹. T-lymphocytes represent an adaptive immune response to injury, requiring the recognition of foreign antigens (peptides, lipids, nucleic acids) in the

presence of inflammatory cytokines for cellular proliferation and immune activation⁶². There are multiple subtypes of T-Cells including effector cytotoxic T-Cells and helper T-Cells that modulate the activity of immune cells through the secretion of cytokines; and regulatory T-Cells (T_{reg}) which suppress the activity of immune cells. As with other immune cells, the number and activity of each of these cells can play beneficial or detrimental roles in SCI.^{63,64}

In SCI, myelin basic protein (MBP) autoreactive T-cells can be found in the serum and tissue of human patients⁶⁵ and experimental animal models^{64,66}. While these autoreactive T-cells were originally believed to induce neurotoxicity, the active transfer of MBP-reactive T-cells and passive immunization with MBP peptide prior to CNS trauma have actually demonstrated a neuroprotective function^{67,68}. Specifically, MBP-reactive T_H1 cells induce a pro-inflammatory environment in rats with SCI while MBP-reactive T_H2 cells polarize the lesion towards an anti-inflammatory environment that improves myelination, neural survival and locomotive scores⁶⁹. T_{reg} cells also play a heterogeneous role in CNS trauma. Their presence in traumatic CNS lesions are capable of suppressing pro-inflammatory responses through the deactivation of the JNK-NF- κ B pathway⁷⁰. However, other studies have shown that their absence improves neuronal survival in optical nerve injury, suggesting they can also augment the immune response negatively⁷¹. Taken together, this suggests that the number and type of T-Cells responding to traumatic CNS needs to be strictly controlled: too few T_{regs} may result in excessive inflammation while too many T_{regs} may suppress the protective effects of autoreactive T-Cells⁷².

1.2.4 Neurotoxicity and Demyelination

Many aspects of secondary injury result in neural or glial necrosis or apoptosis over periods of weeks to months. Free radical formation and extracellular excitatory glutamate

accumulates immediately following SCI and contribute to neural and oligodendrocyte cell death³⁰. Free radical production may result in toxic lipid peroxidation post SCI and therapeutics reducing free radical production are neuroprotective^{73,74}. Apoptosis and necrosis of neurons and oligodendrocytes occur readily as early as 4 hours post injury in rats and continue to as late as 3 weeks post injury³³. In mice, caspase-8 and caspase-3, key initiators of the apoptosis pathway, are significantly increased in mice at days 3 and 7 post injury, timepoints associated with different influxes of immune cells into the lesion⁷⁵. Apoptosis is activated either through extrinsic or intrinsic means. Death receptor FAS/CD95 and its ligand FAS-L/CD95L have been implicated in inducing extrinsic apoptosis through caspase-8 activation⁷⁶⁻⁷⁹.

TNF- α is a pro-inflammatory cytokine capable of inducing neurotoxicity largely through the activation of resident microglia and astrocytes⁸⁰. Neutralization of TNF- α or FAS-L results in diminished neural cell death, reduced inflammatory infiltration and improved functional recovery. Similarly, IL-1 β , which is upregulated in SCI, can initiate apoptosis in neurons and oligodendrocytes through caspase-3 activation⁸¹. Selective inhibition of IL-1 β receptor IL-1R in SCI reduces this apoptotic phenotype⁸²

1.2.5 Glial and Fibrotic Scar

A hallmark of CNS pathology is astrogliosis, in which resident naïve astrocytes become reactive, proliferate, migrate towards the lesion and deposit chondroitin sulfate proteoglycans (CSPGs) and other ECM molecules in the lesion area³². Glial and fibrotic scarring separates healthy tissue from the injury site, restricting inflammation and reducing the spread of tissue damage. Early astrogliosis is marked by STAT-3 dependent migration into the lesion site and protease release that aid in scar formation^{83,84}. A long-held belief in

neuroscience research is that reactive astrocytes prevent axonal regrowth, largely due to the deposition of CSPGs that show an inhibition of neurite growth and remyelination in vitro and in vivo. Supporting this, therapeutic strategies targeting CSPGs, including the use of chondroitinase ABC (ChABC) and xylosides, have shown improved functional recovery in mice and rats⁸⁵. In contrast, full ablation of reactive astrocyte scarring response in mice worsens axonal regrowth across the lesion, identifying that astrocyte responses can be both beneficial and detrimental^{86,87}.

Recent studies have identified heterogeneity in the reactive astrocyte phenotype post injury. Neurotoxic astrocytes are activated by M1 microglia, inducing neurotoxicity both in vitro and in vivo⁸⁸. In addition, these neurotoxic astrocytes secrete an undiscovered pro-apoptotic factor specifically targeting neurons and oligodendrocytes⁸⁸. Beneficial astrocytes have been observed in ischemic models of CNS insult showing distinct transcriptomic signatures and an increased expression of neurotrophic factors that promote functional recovery. This may explain the beneficial effects of STAT-3-dependent astrocyte scar formation mentioned above⁸⁶.

The fibrotic scar comprises acellular proteins secreted by astrocytes, pericytes and perivascular fibroblasts^{89,90}. These cells secrete ECM molecules such as fibronectin, tenascin-C, laminin, collagen and CSPGs in the spinal cord parenchyma, molecules that are normally not expressed in the healthy spinal cord^{31,89}. As with the cellular component, the fibrotic scar may form to help seal the SCI lesion from healthy neural tissue. However, the presence of the thick scar tissue and growth inhibitory ECM molecules presents a physical barrier for severed axons to regenerate⁹¹.

1.3 Granzymes

Granzymes (Gzms) are a family of serine proteases identified within the secretory granules of natural killer (NK) and cytotoxic T-lymphocytes (CTL). These granzymes, in combination with the pore forming protein perforin, play a key role in targeting viral infected or transformed cells for apoptosis^{92,93}. There are five members of the Granzyme (Granule secreted enzyme) family in humans (A, B, H, K and M) and eleven in mice (A, B, C, D, E, F, G, K, L, M and N), each containing a similar His-Asp-Ser catalytic triad responsible for their proteolytic activity⁹⁴. Despite the similar catalytic triad, granzymes vary in their preferred amino acid cleavage site. GzmB is an aspartase, cleaving after aspartic acid while GzmH is a chymase, cleaving after aromatic amino acids (Phe or Tyr)^{95,96}. Both GzmB and GzmH map to chromosome 14. Granzyme A and K are tryptases that cleave after basic amino acid residues (Lys, Arg, Hist) and are located on human chromosome 5 (mouse chromosome 13)⁹⁷. Granzyme M is a metase, preferentially cleaving substrates after methionine or leucine residues and is located on chromosome 19⁹⁷.

Early GzmB research focused on its cytotoxic role in immune-cell mediated apoptosis⁹⁸. Within the last decade a number of novel extracellular activities for GzmB in chronic inflammatory conditions have been identified (reviewed in depth below)⁹⁵. The cytotoxic functions of the remaining granzymes remain an active area of research. GzmH, shows distinct cytotoxic activity similar to GzmB that is not dependent on caspase activation, Bid cleavage to pro-apoptotic truncated Bid (tBid) or the release of cytochrome C from mitochondria, suggesting it is capable of inducing a necrotic form of cell death⁹⁹.

In vitro studies with recombinant GzmA showed a cytotoxic profile distinct from GzmB mediated cell death¹⁰⁰. GzmA is the only protease of the granzyme family that exists

as a dimer of ~52 kDa¹⁰¹. It is responsible for inducing cell death in a caspase-independent manner through the disruption of the mitochondrial electron transport chain, loss of mitochondrial membrane potential, and the generation of ROS⁹². GzmA on its own exhibits significantly less cytotoxic ability than GzmB⁹⁷. In addition to its necrotic function, GzmA is also capable of promoting inflammasome activation and the expression of inflammatory cytokines TNF α , IL-1 β and IL-6 in macrophages in a caspase-1-dependent manner¹⁰².

GzmK shares many similar substrates to GzmA, inducing cell death in target cells in a caspase-independent manner¹⁰³. GzmK has been found elevated in the plasma of sepsis patients and bronchoalveolar lavage fluid of patients with viral infections^{104,105}. GzmK has been shown to bind LPS and potentiates pro-inflammatory cytokine release from monocytes¹⁰⁶. In addition, direct extracellular cleavage of protease activated receptor-1 (PAR-1) upregulates the secretion of pro-inflammatory cytokines from fibroblasts and endothelial cells, highlighting an immune modulating role in chronic inflammatory conditions^{107,108}.

1.4 Granzyme Expression

Granzymes are synthesized with a signal sequence that targets them to the endoplasmic reticulum⁹³. Once inside, this signal sequence is cleaved producing an inactive precursor molecule (ProGzm) that is inhibited by an N-termini dipeptide⁹³. In the Golgi apparatus granzymes are recognized by Mannose-6-Phosphate receptors and shuttled into lysosomes that form secretory granules^{109,110}. Once inside the secretory granules the inhibitory dipeptide is cleaved by cathepsin C (also known as dipeptidyl peptidase I)^{111,112}. Granzymes and perforin are then localized to the electron-dense central core of secretory granules complexed with the chondroitin sulfate proteoglycan serglycin which concentrates

the proteins and prevents their diffusion to the rest of the cell⁹⁵. Granzymes are optimally active at neutral pH, so the acidic environment of secretory granules (pH ~5.5) inhibits and inactivates granzymes, preventing destructive granzyme activity within immune cells^{95,97}.

Granzymes are expressed constitutively in $\gamma\delta$ T Cells, NK T Cells and NK cells. As CD8+ T-cells mature into effector cells from naïve precursors there is an increased expression of GzmA, B and K¹¹³. GzmB and perforin expression can also be induced in CD4+ Th₁, Th₁₇ and T_{reg} cells through TCR engagement and IL-2 signalling^{114,115}. Different groups have further identified GzmB expression in the absence of perforin in other immune cells including macrophages, dendritic cells, regulatory B cells and mast cells¹¹⁶. GzmB can also be expressed in non-immune cells such as chondrocytes, keratinocytes and mast cells¹¹⁶.

1.5 Granzyme B Mediated Apoptosis

Cytotoxic immune cells have two pathways in which they can induce cell death: the death receptor mediated pathway (FAS, FASL binding) or the granule pathway mediated by perforin and granzymes¹¹⁷⁻¹²⁰. Granule-dependent apoptosis is the main mechanism used to eliminate viral-infected or cancerous cells (Figure 2)^{118,121}. Although all granzymes were initially implicated in apoptosis, GzmB is the most potent activator of apoptosis with relatively low concentrations needed to induce cell death *in vitro*¹⁰³. Granule secretion is mediated by the interaction of CTL T-cell receptor with MHC-peptide complexes on the target cell, which leads to the polarization of the microtubule organizing center to the membrane close to the site of the immunological synapse formed between lymphocyte and target cell^{95,122}. Secretory granules fuse with the plasma membrane, releasing their cargo of perforin and granzymes into the immunological synapse. Perforin is a 67 kDa protein capable of oligomerizing into membrane-spanning pores at neutral pH and is dependent on the

presence of Ca^{2+} ^{92,123}. Knockout of perforin in mice results in a decreased ability for T-Cells to induce granule dependent apoptosis, highlighting its crucial role in apoptosis¹²⁴. Perforin synthesis is accompanied with granzyme synthesis when naïve CD8+ or NK cells are activated.

Once inside the target cell, GzmB induces apoptosis through multiple pathways, acting in both the cytoplasm and nucleus of target cells. One major pathway responsible for GzmB-mediated apoptosis is the caspase activation pathway whereby GzmB proteolytically activates pro-caspase-3, resulting in the degradation of cellular components and eliciting apoptosis¹²⁵. GzmB has also been reported to process caspase-8, a major initiator caspase of the apoptosis pathway, in a two-step mechanism involving caspase-3¹²⁶.

GzmB can also activate caspase-3 indirectly through the cleavage of the Bcl-2 protein, Bid^{95,121}. In this case, GzmB cleaves pro-apoptotic Bid into a granzyme-truncated form (gtBid)^{93,121,126}. Similar to the structurally distinct, caspase-8-truncated tBid, gtBid translocates to the mitochondria and facilitates Bax/Bak oligomer formation resulting in mitochondrial outer membrane permeabilization (MOMP) and the release of pro-apoptotic factors such as cytochrome c, Smac/DIABLO, Omi/HtrA2 and apoptosis inducing factor. In particular, cytochrome c release allows for the formation of the apoptosome composed of pro-caspase 9, cytochrome c, and apoptotic protease activating factor-1 (APAF-1) which leads to further downstream activation of caspases-3 and -7. Finally, GzmB cleaves the anti-apoptotic protein Mcl-1, releasing the pro-apoptotic Bcl-2 family member Bim which further contributes to MOMP. Other intracellular substrates for GzmB include Poly ADPribose Polymerase (PARP-1), lamin B, Nuclear mitotic apparatus protein (NUMA), inhibitor of

caspase-activated DNase (ICAD) and tubulin, all of which are also substrates for the effector caspases^{95,121}.

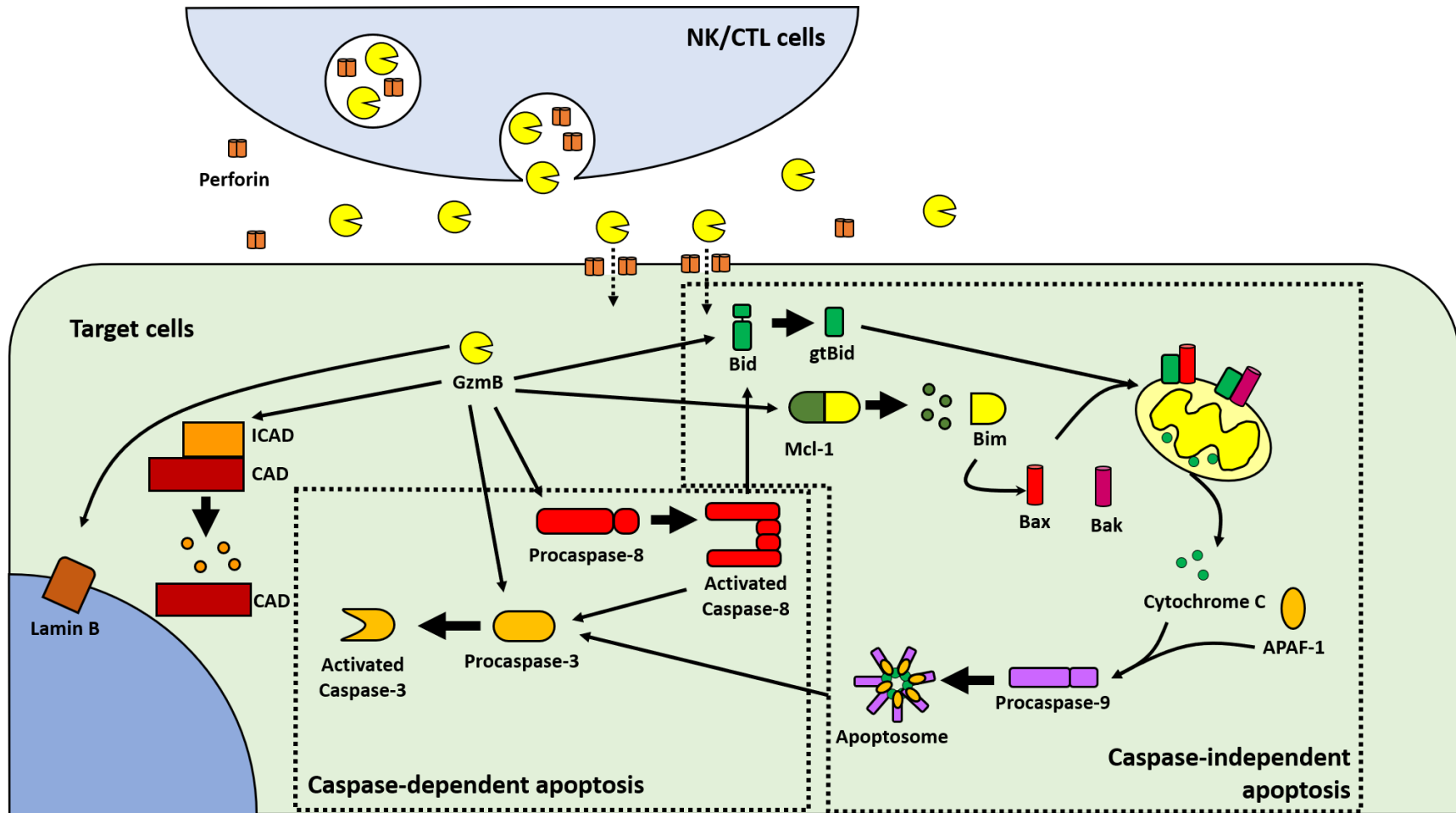


Figure 2 Mechanism of GzmB-Mediated Apoptosis. Schematic of GzmB mediated apoptosis in target viral or transformed cells. GzmB is capable of initiating both caspase-dependent apoptosis through the cleavage of procaspase-3 and -8 or caspase-independent apoptosis through the induction of mitochondrial membrane permeability and apoptosome formation.

1.6 Extracellular Granzyme B

As mentioned above GzmB is expressed in both immune and non-immune cells, including immune cells that lack expression of perforin (ie: basophils, macrophages and mast cells)^{117,127–129}. Furthermore, these cells do not form immunological synapses, suggesting GzmB may accumulate in the extracellular environment. In support of this, many chronic inflammatory conditions have increased GzmB in the extracellular milieu including the synovial fluid of patients with rheumatoid arthritis, the CSF of patients with multiple sclerosis (MS) and the plasma of individuals with human immunodeficiency virus-1 infection or Epstein-barr virus infection^{117,130–133}.

It is not fully known how or why GzmB accumulates in the extracellular environment in these conditions. GzmB may leak from the immunological synapse during CTL target engagement or it may be released non-specifically due to IL-2 activation¹³⁴. GzmB that leaks in this manner are released as both active forms and an inactive zymogen. GzmB could also accumulate from the degranulation of immune and non-immune cells that lack perforin. As there has been no extracellular GzmB inhibitor identified, its proteolytic activity is retained in the extracellular environment¹¹⁰.

A number of novel extracellular GzmB substrates have been identified including fibronectin, decorin, laminin, vitronectin, collagen VII, collagen XVII, $\alpha6/\beta4$ integrin, cadherins, occludins and other cell adhesion molecules^{117,135–137}. Cleavage of these proteins can result in a wide array of different physiological functions. Many of the ECM proteins identified as GzmB substrates play beneficial roles in normal wound healing through tissue remodeling¹³⁸. The cleavage sites for many of these proteins are located in regions crucial for protein-protein interactions, such as the RGD integrin binding domain, which may significantly alter their

adhesive or migratory functions. Laminin, fibronectin and vitronectin, extracellular substrates for GzmB, are associated with the anchoring of epithelial cells to the basement membrane^{139,140}. Cleavage of these proteins can result in a form of detachment-mediated cell death called anoikis, disruption of epithelial or endothelial barrier function or impaired cell migration (Figure 3)^{135,137,141}.

Extracellular GzmB has also been implicated in the processing of cytokines. IL-1 α is a substrate for GzmB and its cleavage results in a protein product that has a higher pro-inflammatory potency than the uncleaved version¹⁴². IL-1 α has multiple biological functions but is typically secreted from dead or dying cells and is implicated in instigating inflammation. The inactive precursor for IL-18 (pro-IL18) can also be activated through cleavage by GzmB¹⁴³.

Finally, substrates for GzmB include VE-cadherin, a protein associated with cell-cell adhesions of endothelial cells¹⁴⁴. Cleavage by GzmB has shown to increase blood vessel permeability and immune cell infiltration in a model of cardiac fibrosis. Cytotoxic T-cells may even use GzmB directly to facilitate transmigration across the basement membrane through the cleavage of ECM proteins such as laminin and vitronectin^{144,145}. Furthermore, GzmB has been shown to increase the bioavailability of vascular endothelial growth factor (VEGF) from fibronectin¹⁴⁶. Increased VEGF activity can lead to an increased vascular permeability that increases immune cell infiltration into injured tissue. TGF- β is an important growth factor involved in cell differentiation, migration and growth and plays important roles in immune-modulation and cancer^{147,148}. Following its secretion, active TGF- β it can be sequestered into ECM such as decorin and biglycan. GzmB has been shown in-vitro to cleave these proteoglycans, resulting in an increased bioavailability of TGF- β ¹⁴⁹.

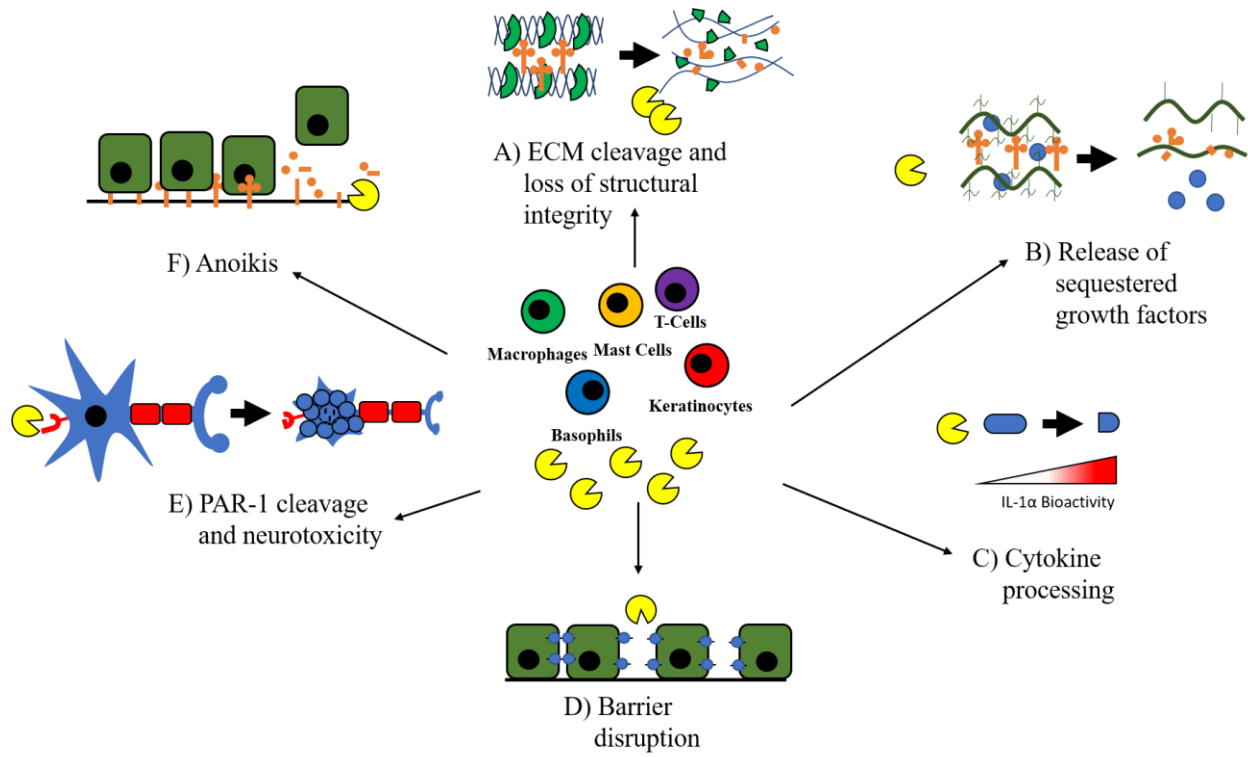


Figure 3 Consequences of Extracellular GzmB Activity. Accumulation of extracellular GzmB can contribute to various phenotypes associated with ECM, cytokine and cell receptor cleavage.

1.7 Granzyme B in Pathology

GzmB expression is increased in many chronic inflammatory conditions. Using transgenic mice lacking the gene for GzmB and selective inhibitors, researchers have been able to identify many roles for GzmB in a number of pathologies involving the immune system and tissue injury. GzmB is associated with the development of abdominal aortic aneurysms (AAA) in mice through the cleavage of fibrillin-1 by immune cells¹⁵⁰. The knockout of GzmB, but not perforin, reduced the incidence of AAA and increased survival, highlighting that the extracellular GzmB function was causing the pathology. Decorin, an ECM protein involved in collagen organization within the adventitia of blood vessels, is another substrate of GzmB that is cleaved during AAA, resulting in a thicker adventitia and less aortic rupture¹⁵¹. Similarly, GzmB is expressed in humans and mice with cardiac fibrosis, and the loss of the immune protease reduces immune cell infiltration, fibrotic scarring and ECM degradation¹⁴⁴.

Cleavage of decorin by GzmB has also been observed in chronic skin inflammatory conditions. In a model of skin aging, GzmB was associated with skin thinning through decorin cleavage and the loss of collagen integrity¹⁵². These aged mice also experienced worsened excisional wound and burn healing rates due to GzmB cleavage of decorin and the fibronectin and vitronectin that is secreted during the formation of granulation tissue^{136,153}. Ultraviolet A (UVA) radiation of keratinocytes induces expression of GzmB *in vitro* and *in vivo*. Chronic exposure to UVA in mice led to GzmB-dependent fibronectin and decorin degradation and collagen thinning^{154,155}. Interestingly, fibronectin fragments generated by GzmB cleavage in photoaged mouse skin were able to induce fibroblast expression of MMP-1, further contributing to collagen loss.

There is an increased GzmB expression in autoimmune diseases such as systemic lupus erythematosus (SLE), scleroderma and type I diabetes¹⁵⁶. Autoimmune disorders result from the immune system mounting a response against itself. In many cases autoimmune conditions are initiated by the creation of cryptic self-epitopes, hidden regions of self-antigens that are exposed following proteolytic cleavage¹⁵⁷. Some of these autoantigens responsible for the development of SLE and scleroderma are cleaved by GzmB during apoptosis. Notably, 21 of 29 well defined autoantigens are directly cleaved by GzmB but not caspase-8 into unique peptide fragments capable of mounting an antibody response in autoimmune patients^{95,158}.

1.8 Granzyme B in Neuroinflammation

Though traditionally understood to be an immune privileged region, many traumatic and immune CNS conditions can increase the permeability of immune cells across the BBB. An example of this is multiple sclerosis, in which focal demyelinating plaques appear in the brain and spinal cord. Cytotoxic T cells, helper T cells macrophages and B cells infiltrate into the CNS in this condition. Demyelination and nerve damage is mediated largely by autoantibodies and the complement system, but immune cells can also secrete numerous cytokines, ROS and nitric oxide species (NOS) that also result in demyelination¹⁵⁹⁻¹⁶¹. Cytotoxic T-cells express GzmB within MS plaques and in experimental autoimmune encephalitis (EAE, the mouse model of MS) and directly use their secretory granules to induce cytotoxicity in human neurons^{160,162,163}. Helper T-Cells also adopt a TH1/17 cytotoxic phenotype in response to IL-15 that is mediated by GzmB and perforin expression¹⁶⁴⁻¹⁶⁶. In fact, GzmB positive cells and extracellular GzmB and GzmA can be found in the CSF of mice with EAE and patients with relapsed remitting MS, suggesting that GzmB may accumulate and function extracellularly within the CNS^{131,166,167}. In addition to

neurons, CTLs are also capable of inducing apoptosis in targeted oligodendrocytes and astrocytes¹⁶⁸.

Self-reactive immune cells in MS are largely derived by myelin associated antigens, specifically MBP, myelin oligodendrocyte glycoprotein (MOG), myelin proteolipid protein (PLP)¹⁶⁹. Transaldolase (TAL) is a protein expressed in oligodendrocytes at high levels. In MS, patients have elevated levels of antibodies against TAL compared to control individuals. GzmB is capable of cleaving TAL, inducing a cytotoxic response from T-cells isolated from MS patients^{170,171}. This suggests that GzmB mediated oligodendrocyte cell death may generate autoantigens (such as TAL) that contribute to pathology in MS.

Extracellular GzmB activity has been implicated in direct neurotoxicity in vitro. GzmB is capable of cleaving PAR-1, a receptor expressed on human neurons¹⁷². Both the supernatant of activated CD8+ T-cells and GzmB alone were able to reduce the viability of cultured neurons mediated by PAR-1 cleavage and voltage gated potassium channel (Kv1.3) expression^{162,172}. This increased neurotoxicity was augmented by IL-1 β , which upregulates PAR-1 expression in neurons. Increased levels of PAR-1 and IL-1 β were identified at the border of demyelinating lesions in MS brain tissue¹⁵⁸. Interestingly, PAR-1 cleavage in neural precursor cells (NPCs) by T-Cell granules reduced generation of neurons while increased the generation of astrocytes (astrogliosis), suggesting extracellular GzmB plays roles both in neurotoxicity and inhibiting neuroregeneration¹⁶⁷. Extracellular GzmB is also capable of entering the cytoplasm of neural cells in a perforin-independent, mannose-6-phosphate receptor-dependent manner¹⁶².

In normal inflammatory conditions, Treg cells are capable of suppressing pro-inflammatory T-cells, resulting in a diminished immune response. Patients with multiple sclerosis exhibit deficits to CD4+CD25+FoxP3+ Treg function of suppressing conventionally

cytotoxic T-Cell responses¹⁷³. One group has shown that extracellular GzmB derived from IL-6 activated non-regulatory CD4+ T-cells inhibits Treg function in an apoptosis-independent manner, adding to the list of extracellular GzmB functions¹⁷⁴.

Research groups have used this GzmB-mediated neurotoxicity as a target for therapeutic development in MS. The administration of serpin3n, an endogenous serine protease inhibitor capable of inhibiting GzmB, to mice with EAE improved clinical scores and decreased the extent of axonal damage and demyelinating in the spinal cord¹⁷⁵. Furthermore, pre-incubation of cytotoxic T-cells with serpin3n attenuated the in vitro cytotoxic effects on neurons. Taken together this supports the therapeutic potential of GzmB inhibition in neuroinflammatory conditions.

Neurotoxic lymphocytes are also a major mediator of disease in amyotrophic lateral sclerosis (ALS). ALS is a disease characterized by the loss of upper and lower motor neurons of the motor cortex, brainstem and spinal cord^{176,177}. The formation of protein-rich inclusions within the cell body of motor neurons predicates their death. Resident microglia and astrocytes become activated in response to the misfolded proteins. Pro-inflammatory CD8+ T-Cells, Th1 and Th17 cells infiltrate into the CNS and secrete inflammatory cytokines and cytotoxic molecules, including GzmB and perforin, that are believed to induce neuron death. In support of this, there is an increased expression of GzmA and GzmB in the serum of patients with ALS¹⁷⁸.

The role of GzmB in traumatic CNS injury is poorly understood. As mentioned above, traumatic brain or spinal cord injury involves a large immune component that includes the infiltration of T-cells into the CNS. One group identified an increased level of GzmB in the SCI tissue of rats which peaked at 3 days post injury¹⁷⁹. GzmB expression was colocalized with neuronal-specific enolase (neuronal marker) and TUNEL (apoptosis marker), identifying GzmB

as a neurotoxic agent in traumatic SCI¹⁷⁹. To my knowledge no studies have identified a role for GzmB in traumatic brain injury (TBI). Other neurological conditions that involve GzmB+ immune cell infiltrate include vasculitis neuropathy, rasmussen's encephalitis, sensory perineuritis, cerebral ischemia and experimental cerebral malaria^{95,180}.

1.9 Rationale and Hypothesis

Traumatic SCI are wounds to the CNS that involve inflammatory responses that do not resolve themselves in a way that skin or muscle wounds do, resulting in chronic inflammation. This immune response is characterized by resident microglia and astrocyte responses as well as infiltrating neutrophil, macrophage, and T cells (cytotoxic, helper and regulatory)^{33,34}. Previous studies have identified that GzmB contributes to neural apoptosis in rat SCI, however the mechanisms by which GzmB contributes to tissue damage and subsequent motor or sensory deficit in mouse SCI are not understood¹⁷⁹. Inhibition of GzmB activity in a murine model of EAE results in reduced demyelination and less axonal damage, suggesting that targeting GzmB in neuroinflammatory conditions may be a viable therapeutic option.

GzmB is also implicated in increasing vascular barrier permeability. SCI have increased BBB permeability that allows blood proteins and immune cells to enter the spinal cord lesion with less effort. Chronic expression of GzmB in the SCI lesion may also contribute to increased vascular permeability and prolonged inflammation, resulting in reduced neurogenesis and increased neurotoxicity.

Mice subjected to a thoracic-level SCI show robust paralysis of the hindlimbs with a reproducible recovery timeline¹⁸¹. Many studies have been performed investigating the therapeutic benefit of immunomodulatory therapy, be it inhibition or treatment with pro- or anti-inflammatory cytokines or the conditional knockout of specific immune factors. Thoracic SCI

models provide us with a standardized, reproducible means to investigate locomotive recovery and neuroprotective benefit of the knockout of GzmB.

I *hypothesized* that GzmB deletion in mice will improve locomotive recovery following SCI by reducing the loss of neurons, oligodendrocytes and myelinated axons.

My specific aims were:

1. To compare the locomotive recovery of GzmB KO versus WT mice following SCI.
2. To identify the cellular source(s) of GzmB in murine SCI.
3. To assess demyelination and neural cell loss in GzmB KO vs. WT mice.

Chapter 2: Materials and Methods

2.1 Mice

Male C57Bl/6 (12-16 weeks old, Jackson Laboratories, referred to as wild-type or WT) and GzmB KO mice (12-16 weeks old, purchased through Jackson Laboratories and bred in facility) were housed and maintained in the animal vivarium of the International Collaboration of Repair Discoveries (ICORD). Animal experiments were performed in compliance with requirements of the Canadian Council on Animal Care and the University of British Columbia Committee on Animal Ethics.

2.2 Spinal Cord Contusion Injury

Spinal cord injuries were performed following a standardized protocol¹⁸². Briefly, mice were anesthetized with 2.5% isoflurane in 100% oxygen and placed onto an electric heating pad to maintain body temperature. Once anesthetized, animals had their back shaved, cleaned and sterilized with Hibitane and 70% ethanol. Mice were injected with 1.0 mL of Ringer's Saline and 0.1 mg/kg buprenephrine to reduce post-operation dehydration and pain, respectively. A trained surgeon performed a laminectomy by first splitting the midline of the back, exposing the vertebral column. The dorsal laminae of thoracic vertebrae 9 and 10 were removed with fine rongeurs, exposing the spinal cord. Mice was centered below the impact tip of the Ohio State University (OSU) Impactor Device and a T9 contusion injury was induced by dropping a weight and controlling for the force of impact at 70 kDynes. The animal was then closed with simple interrupted sutures at both the muscle and skin layer and transferred to a heated recovery cage. Mice were monitored daily for signs of pain, weight loss/gain, and the development of secondary complications (bladder infections, foot necropsy etc.) Buprenorphine was administered every 8 hours for 3 days following injury. Mice were separated into two cohorts i) a short-term group (7

days post injury) to investigate inflammatory cytokine and GzmB expression and **ii**) a long term group (42 days post injury) to investigate locomotive recovery and tissue damage. Two further groups of WT and GzmBKO mice were not subjected to the spinal cord injury above. Spinal cord tissue was isolated for qPCR and histology controls.

2.3 Mouse Behavioral Tests

Animal locomotive recovery was assessed in the long-term group only using three separate behavioral tests: 1) the Basso Mouse Scale (BMS), 2) rotarod, and 3) horizontal ladder test as described below. An open field locomotion test using the BMS was performed at days 2, 5, 7, 9, 14, 21, 28, 35 and 42 post injury while the rotarod and horizontal ladder tests were conducted at days 14, 28 and 42 post injury (Figure 4).

2.3.1 Basso Mouse Scale

Open field locomotion was assessed using the BMS, an open field test that assigns a score to each animal's hindlimb motion ranging from 0 to 9 (0 = complete hind limb paralysis, 9 = normal locomotion)¹⁸¹. All observations were performed in a clear 92 cm x 122 cm plexiglass container by two observers blinded to the experimental groups. One observer acted as the “recorder”, taking notes on the visual observations made during the test. The other observer acted as the “lead”. The “lead” observer gave each mouse a final score based on comments made from both observers. The “lead” and “recorder” observers remained the same over the course of the study. Mice were acclimatized to the experimental apparatus for 4 minutes on three separate days prior to baseline measurements. Any mouse that scored less than 8 in their baseline measurement was removed from the experimental group. The final score represents the mean of each animal's left and right hindlimb score. BMS subscore, which provides a cumulative score of

positive gait characteristics (i.e.: parallel paw rotation, coordinated stepping, trunk stability), was scored on a scale from 0-11 based on observations made for the general BMS score.

2.3.2 Rotarod

A murine rotarod was used to assess muscle endurance, motor coordination, balance and grasp following SCI and was performed as previously described¹⁸³. Briefly, mice were placed on the rotarod set initially to rotate at 4 rpm. After 10 seconds the machine began to accelerate at 20 rpm/min to a maximum speed of 40 rpm and ran until the mouse fell off. The final rotation speed and time was recorded. This was repeated for a total of 3 trials per timepoint. If the mouse fell off between 0 and 5 seconds the fall was likely due to poor placement on the rotarod and was not counted as a trial. If the mouse fell off between 5 and 10 seconds (prior to acceleration) the final speed and time for that trial is 4 and 0 respectively. Mice were trained on the rotarod for at least 5 days prior to baseline measurement.

2.3.3 Horizontal Ladder Test

The horizontal ladder test was conducted as previously reported¹⁸⁴. A horizontal ladder with dimensions length 60 cm x width 4 cm x height 60 cm contained 50 metal horizontal ladder beams spaced 1.25 cm apart and at a height of 30 cm above the bottom of a plexiglass chamber. Mice performed baseline recordings once every 14 days post injury up to 42 days. For each recording, mice were placed in an escape cage containing bedding from their home cage at the end of the apparatus. After acclimatizing for at least 3 minutes mice are placed at the beginning of the ladder apparatus and allowed to run back towards the escape box on their own. At least 3 passes were recorded per timepoint ensuring the mice traveled along the ladder at constant speed without pausing or reversing direction. The first 3 successful passes without pauses were selected for video analysis for each timepoint.

Video analysis was performed by two analysts blinded to the mouse conditions. Each rung was scored based on how the mouse's hindlimb stepped past it: positive steps include normal plantar grasping of the rung (Plantar), contact of the rung by only the toes (Toes), or by entirely passing above the rung (Skip) while negative steps include the hind-paw slipping past the plane of the beams after contacting the rung (Slip), the hind-paw missing the rung entirely and passing through the plane (Miss), or the dorsal side of the hind-paw dragging against the rung (Drag)¹⁸⁵. If a mouse performs a negative step while contacting a rung (ie: a slip), the rung was given a score of 1. If a mouse performs a negative step in between two rungs (ie: a miss), the lower-numbered rung was given a score of 1. If a mouse does not perform a negative step, the rung was given a score of 0. Data are represented as % missteps by taking the sum of rung scores for both hindlimb and dividing that by the total number of steps (60) per run. Data was averaged between the two analysts.

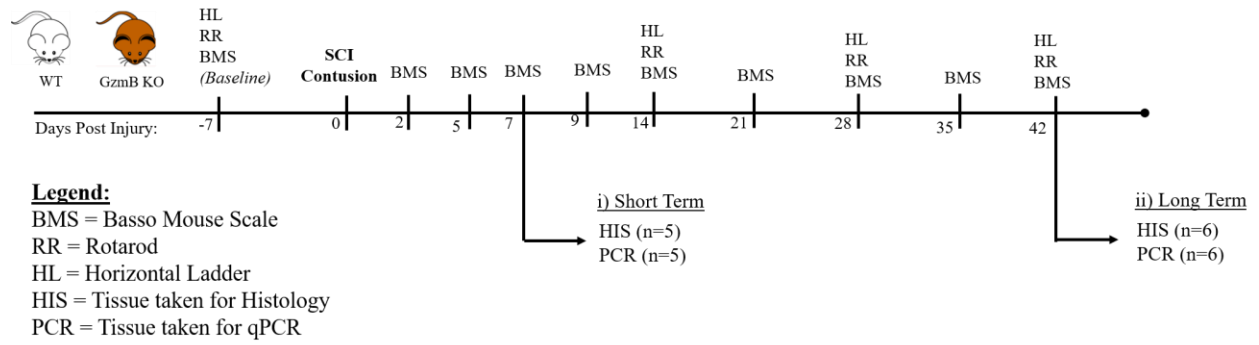


Figure 4 Mouse SCI Study Timeline. Timeline of behavioural tests and endpoints for the mouse study.

2.4 Animal Sacrifice and Tissue Processing

At the end of each timepoint (7 or 42 days post injury), animals were sacrificed *via* a terminal anesthetic dose of chloral hydrate (100 mg/kg, i.p). Half of the mice in each timepoint were randomly sorted for analysis *via* qPCR group or Histology group (n=6 each). For the qPCR group the animals were trans-cardially perfused with 20 mL of chilled phosphate buffered saline (PBS) for 10 minutes (2mL/min) to clear the spinal cord of blood cells. 5 mm of spinal cord centered around the lesion was removed with a scalpel, flash frozen in liquid nitrogen, and stored at -80°C. For the histology group the animals were trans-cardially perfused with PBS followed by 20 mL of 4% paraformaldehyde fixative solution for 10 min. 5 mm of spinal cord centered around the lesion was removed, placed in a tissue cassette and post-fixed in 4% paraformaldehyde for at least 4 hours to ensure full tissue fixation. Spinal cords were then incubated in sucrose gradient solutions of 12%, 18%, and 24% (each for 24 hours) to cyroprotect the tissue. Segments were then placed in Tissue-Tek® optimal cutting temperature (OCT) embedding medium, frozen over dry ice and stored at -80°C. Spinal cord lesions were serially sectioned into 20 µm cross sections on a cryostat at -20°C and stored at -80°C prior to immunohistochemical staining. Uninjured WT and GzmB KO mice were similarly harvested for histology and qPCR.

2.5 Eriochrome Cyanine Myelin Staining

Eriochrome Cyanine (EC) stain was prepared by adding 0.08 g EC in 40 mL of dH₂O with 200 µL H₂SO₄. 2 mL of 10% FeCl₃ was added and the solution was topped up to 50 mL before filtering into a light protected bottle. Slides were allowed to thaw at room temperature for 1 hour. Sections were incubated in xylene followed by gradual rehydration in decreasing ethanol gradient solutions (100%, 100%, 90%, 70%, 50%) before washing in dH₂O. Slides were then

incubated in EC stain for 10 mins followed by two washes in dH₂O. The dye was then differentiated by incubating in 0.5% NH₄OH for 1 minute (to allow for a visible color change between the gray and white matter) followed by dH₂O washes. Slides were then dehydrated in increasing alcohol content solutions before mounting with xylene based mounting media (Cytoseal 60, Thermofisher).

2.6 Immunohistochemistry

Sectioned spinal cords were removed from the -80°C freezer and allowed to defrost for 1 hour at room temperature. Once thawed, slides were outlined with Dab Pen to create a hydrophobic barrier surrounding the tissue. Slides were rehydrated in 0.1 M PBS for 10 minutes to wash away OCT medium. Slides were permeabilized for 10 minutes with 0.1% PBS-Triton X-100 and blocked in 10% normal Donkey Serum in 0.1% PBS-TritonX100 (blocking buffer) for 30 minutes. Slides were incubated overnight with primary antibodies diluted in blocking buffer (Table 1). The next day the slides were washed (3x 5 minutes each in 0.01 M PBS) and incubated for 2 hours in the dark in blocking buffer containing secondary antibodies raised conjugated to Alexa fluorophores (488 nm, 594 nm). After another round of washes slides were incubated in PBS containing DAPI for 10 minutes at room temperature in the dark and coverslips mounted using EMS HydroMount (Fisher). Stained slides were stored at 4°C until imaging.

Table 1 List of Antibodies and Reagents

Antibody	Manufacturer (Cat #)	Dilution	Animal Raised in
1° Antibodies			
CD68	Bio-Rad (MCA1957)	1:100	Rat
GzmB	Abcam (Ab4059)	1:200	Rabbit
NeuN	Abcam (ab177487)	1:300	Rabbit
2° Antibodies			
Anti-Rabbit 488	Thermofisher (R37118)	1:500	Donkey
Anti-Rabbit 594	Thermofisher (A-21207)	1:500	Donkey
Anti-Rat 488	Thermofisher (A-21208)	1:500	Donkey
Miscellaneous			
DAPI	Thermofisher (D1306)	1:2500	N/A

2.7 RNA Extraction and qPCR

RNA was extracted from flash frozen spinal cord lesions using TRIzol® reagent (Thermo Fisher) as per manufacturers' protocol. Briefly, 0.5 mm of spinal cord tissue centered around the lesion was homogenized in 1.0 mL Trizol using a TissueLyser LT (Qiagen). Tissue pieces were homogenized with 5 mm stainless steel beads for 3 minutes at 50 Hz. Lipids (from myelin sheaths) were separated by centrifuging the lysate at 12,000 x g for 10 minutes at 4°C. Following this 200 µL of chloroform was added, mixed by hand for 15 seconds and centrifuged at 12,000 xg for 15 minutes at 4°C. The top aqueous layer containing RNA was moved to a new 1.5 mL microtube. 500 µL of isopropanol was added to the aqueous layer and incubated for 10 minutes at room temperature to precipitate RNA. RNA was then pelleted by centrifugation at 12,000 xg for 10 minutes at 4°C and the pellet washed with 75% ethanol. RNA was pelleted by centrifugation at 7,500 xg for 5 minutes at 4°C and the pellet air dried for 10 minutes at room temperature. Dried pellets were resuspended in 50 µL of nuclease-free H₂O. Contaminating DNA was removed from RNA by incubating 5 µg of RNA sample with DNase I (New England Biosciences) at 37°C for 10 mins followed by 85°C for 10 mins to inactivate the enzyme. cDNA was synthesized from 1 µg of DNase-treated RNA using reverse transcriptase, random hexamers and dNTP master mix from Invitrogen. cDNA was synthesized by incubating reagents at 42°C for 30 minutes followed by 95°C for 10 mins. PCR amplification was performed using SYBR green (Applied Biosystems) on an Applied Biosystems ViiA 7 real-time PCR system under the following conditions: Phase 1 50°C, 2 mins. 95°C, 5 mins. Phase 2 95°C 15 secs, 60°C 30 secs, repeat x40. Phase 3 60°C to 95°C at 0.05°C/sec. Primers were used at a final concentration of 0.4 µM (Table 2).

Table 2 List of Primers Used for Genotyping and qPCR

Gene	Direction	Sequence (5'→3')
Genotyping		
GzmB	Forward	CTGCTACTGCTGACCTTGTCT
	Reverse (WT)	TGAGGACAGCAATTCATCTA
	Reverse (KO)	TTCCTCGTGCTTTACGGTATC
qPCR		
GAPDH	Forward	TGCACCACCAACTGCTTAGC
	Reverse	GGCATGGACTGTGGTCATGAG
TNF- α	Forward	GGGGCCACCACGCTCTTCTG
	Reverse	GGGCTACAGGCTTGTCACCTCG
IL-1 β	Forward	GCAACTGTTCCTGAACTCAACT
	Reverse	ATCTTTTGGGGTCCGTCAACT

2.8 GzmB KO Genotyping

Ear clips were taken from mice during weaning and were incubated in 100 uL of 25 nM NaOH, 0.2 mM EDTA at 95 °C for 10 minutes. 100 uL of 40 mM Tris-HCl, pH 5.0 was added with vortexing to extract DNA from the tissue. DNA was amplified using TopTaq master mix (Qiagen) using the primers listed in Table 2. Reactions were run in a thermocycler (BioRad T-100) using the following conditions: Step 1: 94 °C, 3 mins. Step 2: 94 °C 30 secs, 66 °C 1 min, 72 °C 1 min, repeated 35 times. Step 3: 72 °C, 2 mins.

2.9 Image Analysis

Slides stained with EC were imaged with an Aperio CS2 Slide scanner (Leica). Total amount of white matter was quantified in ImageJ by a blinded analyst by manually outlining the blue (myelin positive) regions. Sparing white matter was expressed as a ratio of total lesion area for each spinal cord section. In each animal, the segment that had the smallest white matter sparing ratio was designated as the epicenter of the lesion.

Slides stained against NeuN (marker for neurons) were imaged at the epicenter (as defined above) and up to 600 μm rostral or caudal to the epicenter. Regions were imaged at 350μm x 350μm centered at the dorsal horn. Both dorsal horns of each cord segment were imaged and NeuN positive cells were manually counted by two blinded analysts with ImageJ. Data are represented as the sum of total dorsal horn neurons averaged between the two analysts.

2.10 Statistical Analysis

All data are represented as the mean \pm standard deviation. Mouse behavioral studies and spinal cord lesion tissue damage (Myelin and neuron quantification) were analyzed by two-way ANOVA followed by a Fisher's multiple comparison test. Survival data was analyzed by the Mantel-Cox method. Injury parameters were analyzed by Mann-Whitney U-test. *P*-values are

represented as follows: * $p < 0.05$ ** $p < 0.01$ *** $p < 0.001$. All statistical analysis was performed using GraphPad Prism version 7.0 (GraphPad Software, San Diego, California).

Chapter 3: Results

3.1 Spinal Cord Injury Parameters and Survival

In both the short term (7 days) and long term (42 days), cohorts did not exhibit significant differences in injury velocity ($p_{\text{long}}=0.6213$ and $p_{\text{short}}=0.639$), displacement ($p_{\text{long}}=0.519$ and $p_{\text{short}}=0.8413$) or force ($p_{\text{long}}=0.6904$ and $p_{\text{short}}=0.7153$), confirming the reproducibility of these injuries (Figure 5C-H). Generally, mice survive moderate spinal cord injuries and suffer only minor injuries or morbidities¹⁸⁶. Of the two cohorts, only the long-term study had mice that had to be sacrificed prior to the study end point due to complications (i.e bladder infection, foot necrosis) that arose during their recovery. However, there was no statistical difference ($p = 0.121$) in survival between the groups (Figure 5 A, B).

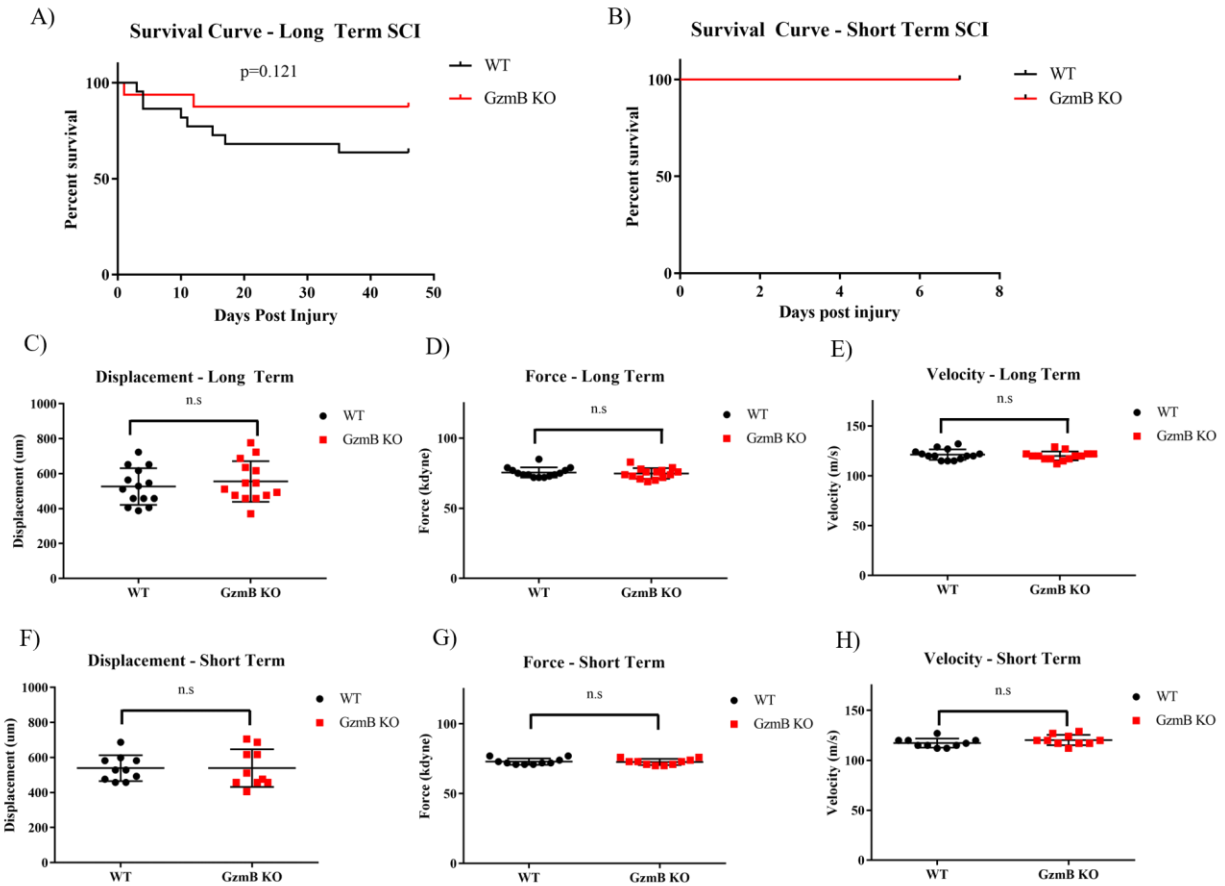


Figure 5 Injury Parameters. Survival curves for WT and GzmB KO mice for the long (A) and short (B) term studies. Displacement (C, F), force (D, G) and velocity (E, H) graphs for the long- and short-term cohorts respectively. $n=14$ for the long-term study (A, C-E) and $n=10$ for the short term study (B, F-H). n.s. = not significant $p > 0.05$.

3.2 Locomotive Recovery is Improved in GzmB KO Mice

GzmB KO mice showed a significantly improved BMS score at 35 ($p=0.0480$) and 42 weeks ($p=0.0114$) post-injury compared to WT mice (Figure 6A). The BMS sub-score showed no significant difference between WT and GzmB KO mice at any point during recovery (Figure 6B).

GzmB KO mice showed significantly better rotarod scores at 14 ($p=0.0404$) and 28 days ($p=0.0400$) post injury but their scores lost significance by 42 days ($p=0.2399$) (Figure 6C). Rotarod scores did not significantly improve over the 42-day recovery period in either group. GzmB KO mice performed significantly better than WT mice at the Horizontal Ladder task at all time points ($p_{14 \text{ days}}=0.004$, $p_{28 \text{ days}}=0.0004$, $p_{42 \text{ days}}=0.0212$) and, like the rotarod, neither group showed any improvement over time (Figure 6D).

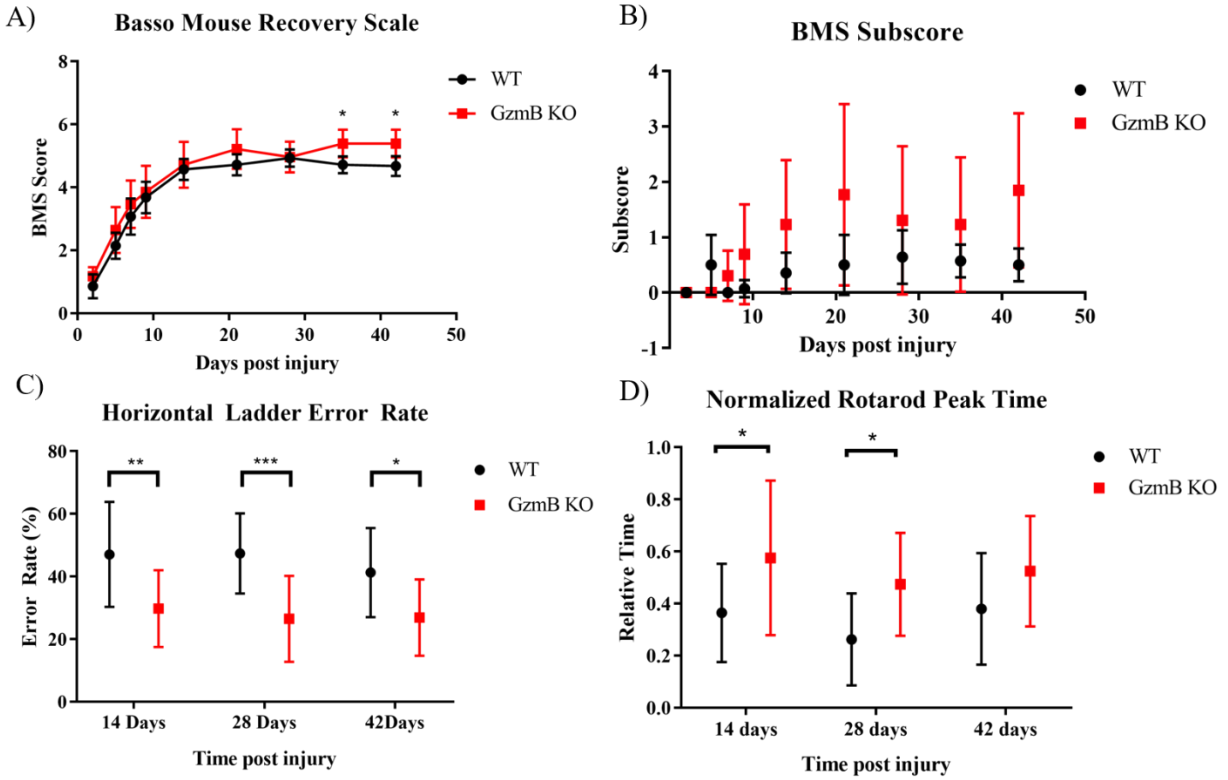


Figure 6 Locomotive Function After SCI is Improved in GzmB KO Mice. GzmB KO mice showed improved locomotive scores in the BMS (A), Rotarod (C) and Horizontal Ladder (D) tests but not the BMS Subscore (B). n=14, * p<0.05, ** p<0.01, *** p<0.001.

3.3 Expression of GzmB in Mouse SCI

Staining of SCI lesions from WT mice 7 days post-injury demonstrated that GzmB localized to distinct, granular-like regions of CD68-positive macrophages or microglial cells (Figure 7C, D). As expected, GzmB appears granular within the cytoplasm of these cells, suggesting they are part of secretory granules (white arrows). There was no expression of GzmB in CD68+ cells of uninjured spinal cord (Figure 7A, B) or in the lesions of GzmB KO mice (Figure 7E, F). Not all CD68+ cells within the spinal cord lesion expressed GzmB.

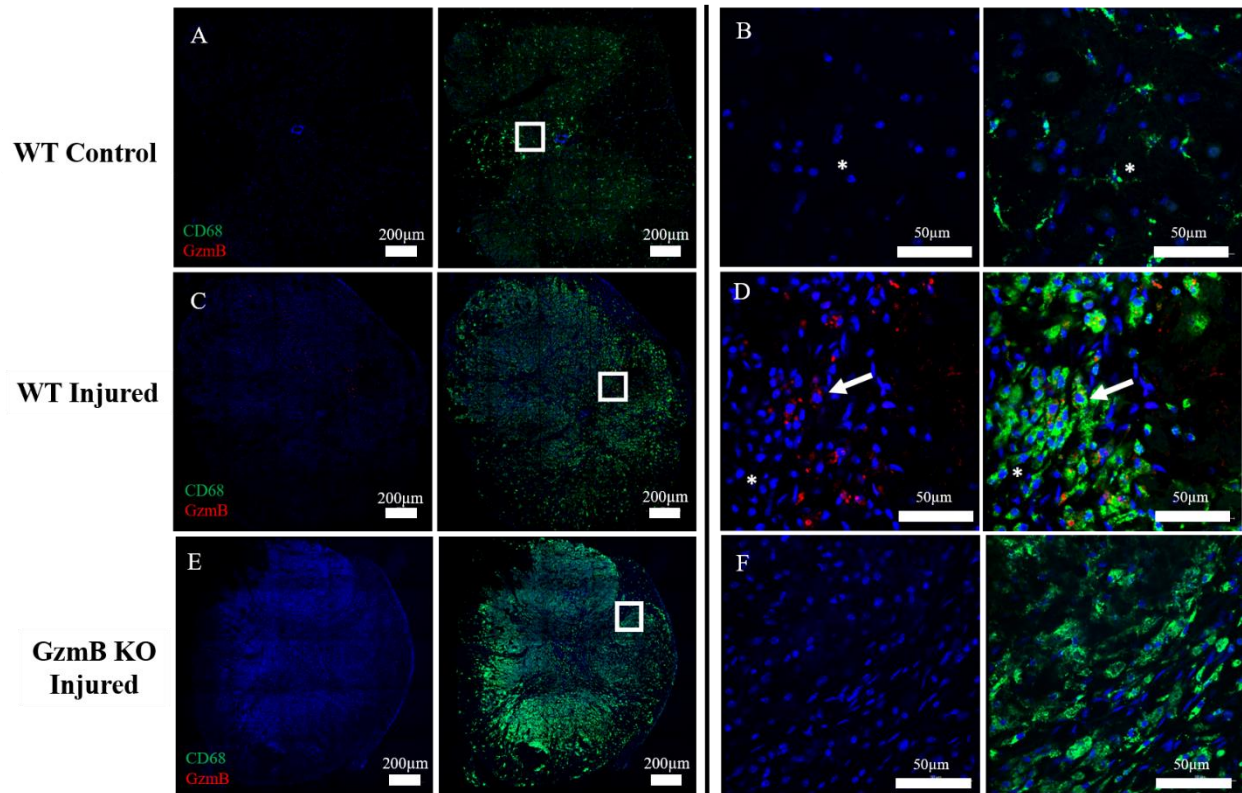


Figure 7 GzmB Expression in Mouse SCI Lesions. GzmB (red) expression within uninjured (A: 20x stitching, B: 40x) and injured WT (C: 20x stitching, D: 40x) and GzmB KO (E: 20x stitching, F: 40x) mice. White boxes in A, C and E represent the region of the spinal cord that is imaged in B, D and F. DAPI was used to counterstain nuclei. Images shown are representative of results obtained from 6 individual mice per genotype for injured mice and from 3 individual mice per uninjured mice.

3.4 Preservation of White Matter in GzmB KO Mice Following SCI

To evaluate the extent of damage within the spinal cord following SCI we investigated the presence of myelin across the SCI lesions using eriochrome cyanine R. GzmB KO mice demonstrated an increase in total area of myelin-positive staining (blue) at the epicenter and rostral, but not caudal, to the lesion compared to WT mice ($p_{-400}=0.0077$, $p_{-200}=0.0001$, $p_{\text{epicenter}}=0.0203$) (Figure 8A, B). The increased myelin positive area in GzmB KO animals suggests that there is a higher percentage of intact myelinated axons and less demyelination which may be a result of the lack of GzmB in the injured region.

3.5 Increased Neuron Survival Across SCI Lesion in GzmB KO Mice

A second hallmark of SCI secondary injury is immune cell mediated apoptosis³³. We investigated the survival of neurons in the dorsal horn of spinal cord segments across the lesions at 6 weeks post injury. A GzmB KO mice showed a larger number of NeuN positive nuclei at both rostral and caudal regions of the lesion ($p_{-600} = 0.0016$, $p_{400} = 0.0149$, $p_{600} = 0.0195$) (Figure 8C).

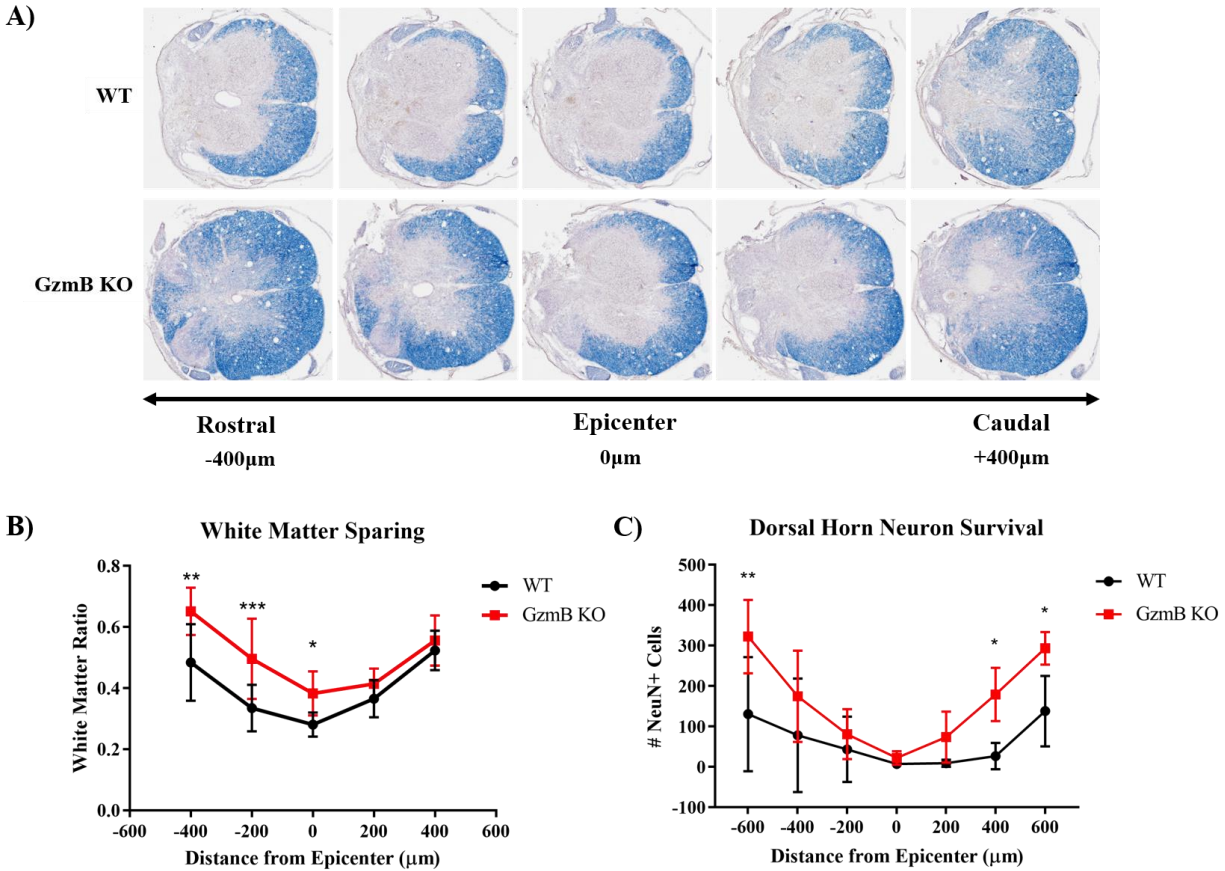


Figure 8 White Matter Myelin and Neuron Survival is Increased in GzmB KO Mice Post-Injury. Representative images (A) and graph (B) of myelin sparing for WT (top) and GzmB KO mice (bottom). Dorsal horn neuron survival count of GzmB KO mice from rostral to caudal (C). n = 6 mice per genotype.

3.6 Lack of GzmB Does not Influence Pro-Inflammatory Cytokine Expression

Expression of pro-inflammatory cytokines may cause an increase in tissue damage post-injury^{77,82}. Using qPCR we quantified the transcript levels of the pro-inflammatory cytokines TNF- α and IL-1 β . There was no difference in TNF- α or IL-1 β mRNA expression 7 days post-injury (Figure 9A, B).

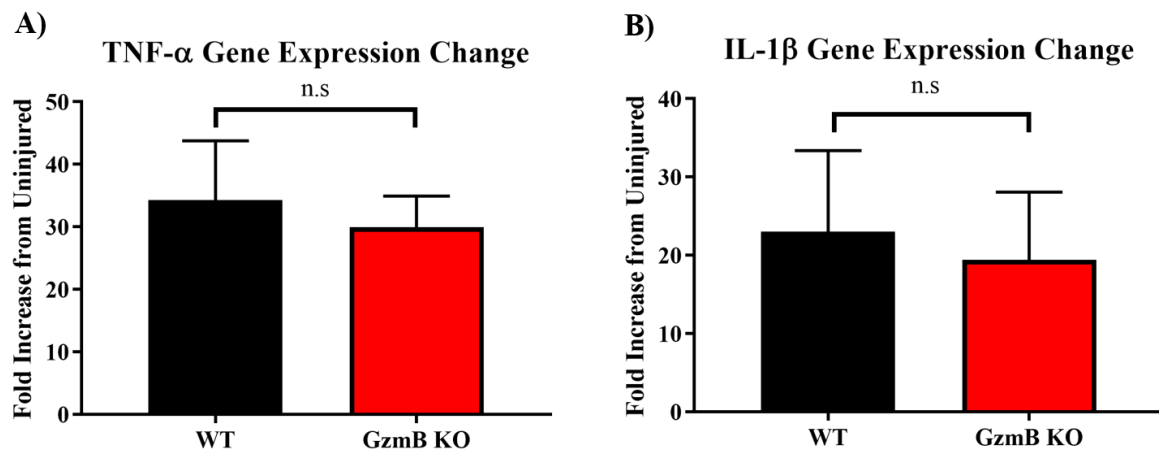


Figure 9 IL-1 β and TNF- α mRNA Expression GzmB KO and WT Mice Post-SCI. Spinal cord lesions showed no significant change in mRNA transcripts for TNF- α (A) or IL-1 β (B) 7 days post-injury. n=5 mice per genotype. n.s = not significant ($p > 0.05$).

Chapter 4: Discussion

Traumatic SCI results in immediate neuron and oligodendrocyte death at the epicenter of the injury. Many immune-cell secretions, including cytokines and proteases, contribute to neurotoxicity. GzmB has previously been investigated as a protease affecting wound healing in chronic skin, vascular and neuroinflammatory conditions^{136,175}. However, there has been no research to date on the potential therapeutic benefit of inhibiting or deleting GzmB expression within SCI. In this study, a thoracic contusion injury model was selected to investigate the benefit of GzmB deletion in mice. A contusion injury was selected over other models of SCI, such as spinal cord transection, ischemia/reperfusion or compression injuries, as contusions are generally more clinically relevant and involve larger inflammatory responses¹⁸⁷. The injury parameters were selected to mimic a “moderate” injury pattern in mice (50-70 kdyne force, ~500 μ m displacement) that is frequently used in mouse SCI research^{89,188,189}.

While the spinal cord injury model is set to be reproducible between animal groups, many labs have reported markedly different recovery timelines in C57Bl/6 mice subjected to a moderate injury (as shown by their BMS scores). While investigating the effects of treatment of anti-inflammatory cytokine IL-33 in mice post SCI, Pomeschchik et al performed a 60 kdyne T-9 contusion in C57Bl/6 mice in which both vehicle and cytokine treated groups only recovered to 2.5 (extensive ankle movement and occasional plantar placement) and 3.5 (Plantar placement and occasional plantar stepping) respectively^{181,190}. Final BMS scores of approximately 3 (Plantar placement only) are regularly seen in the control group of C57Bl/6 mice of many other groups^{181,191–194}. On the other hand, H. Li et al performed a mouse SCI with a 60 kdyne impact that showed mice recovering to an average score of 7 (Consistent coordinated plantar stepping, occasional parallel paw rotation)^{181,189}. In this study, mice consistently recovered to a BMS score

of 4.5 (WT, occasional or consistent plantar stepping, no coordination) or 5.5 (GzmB KO, consistent plantar stepping, some coordination)¹⁸¹. This suggests mouse recovery may be dependent on factors specific to different animal facilities (i.e. inconsistent measurements of the forces, microbiome, post-operative care, mouse strains, diet).

Because of the conflicting reports associated with BMS, two other tests were added to assess motor function. Utilizing the rotarod and horizontal ladder test we were able to detect significant increased skilled locomotor function of GzmB KO mice compared to WT immediately after injury. Notably, the rotarod and horizontal ladder were able to pick up differences in skilled locomotor function at early timepoints that were not identified with the BMS. This may be due to the rotarod and horizontal ladder tests increased sensitivity in determining fine locomotor skills compared to the open field BMS test. These data agree with the results reported by other labs from experiments that have inhibited extracellular proteases. For example, MMP-3, -9 and -12 increase secondary injury by increasing vascular permeability, and their respective knockouts significantly improve locomotive scores while reducing immune infiltration⁴¹⁻⁴³. In addition, inhibiting MMP-2/9s have shown to be beneficial for functional recovery¹⁹⁵. Treatment of rat SCI with less specific protease inhibitors, such as Minocycline or the serine protease inhibitor Nafamostat, also results in improved functional recovery, as measured by the Basso-Beattie-Bresnahan scores^{196,197}.^{196,197}.

The expansion of tissue damage and paralysis following SCI can be a result of neuron death and myelin loss during secondary injury cascades. Studies with therapeutics that reduce the extent of cell death within the spinal cord, such as TNF- α antagonists or methylprednisolone, show that increased cell survival correlated with an improved locomotive function^{77,198}. To assess whether the locomotive improvements seen in this study could be the result of decreased

neuron cell death, we quantified the number of surviving neurons in the dorsal horns across the lesion. GzmB KO mice showed increased neural cell counts compared to the WT group. This supports previous studies that show that GzmB can induce apoptosis in neurons extracellularly or intracellularly^{172,179}. Directly reducing neural apoptosis during secondary injury, for example through the inhibition of GzmB activity, is an attractive therapeutic target in SCI as reduced neural cell death results in improved locomotive recovery *in vivo*^{77,78}.

Demyelination of axons following SCI is a result of extensive oligodendrocyte cell death, which may be promoted by multiple mechanisms including mechanical trauma, glutamate excitotoxicity¹⁹⁹ cytokine signaling²⁰⁰, hemorrhage²⁰¹ or immune cell interactions. After the initial trauma there is a chronic progressive demyelination phenotype that may be caused by autoreactive T-lymphocytes^{69,202}. Here we show that the deletion of GzmB, a protease traditionally associated with cytotoxic T-cells, results in an increase in white matter sparing post SCI. It's important to note that the loss of myelin in spinal cord white matter after injury may be due to oligodendrocyte cell death or a by-product of axonal cell death. A role for GzmB in demyelination is supported by Haile et al, who showed a similar sparing of white matter in mice treated with a murine specific extracellular GzmB inhibitor (Serpina3n) in a model of EAE¹⁷⁵. GzmB has also been implicated in perforin-dependent T-cell mediated oligodendrocyte cell death in brain slice cultures²⁰³. Interestingly, in these experiments, oligodendrocyte-reactive T-cells were capable of inducing neuronal death, which was believed to be due to leakage of GzmB and perforin out of the immunological synapse.

Following SCI, dying oligodendrocytes can be replaced by the differentiation of oligodendrocyte precursor cells (OPCs) into mature, myelinating oligodendrocytes²⁰⁴. Successful remyelination of axons by newly-derived oligodendrocytes is dependent on the level of

stimulatory vs. inhibitory factors expressed within the lesion. TNF- α , myelin debris and glial scar proteins have all been implicated in inhibiting OPC migration and differentiation into oligodendrocytes²⁰⁵. Targeting these negative factors have corresponded to higher Reports have also identified that OPCs express PAR-1, and its activation by serine proteases results in decreased OPC differentiation and expression of myelin-associated genes²⁰⁶. While no studies have been conducted on the effects of GzmB activation of PAR-1 in OPCs, it presents a possible mechanism for the increased myelin staining of GzmB KO vs. WT mice.

We next attempted to identify the immune infiltrate contributing GzmB expression within the spinal cord lesions. While GzmB is classically associated with cytotoxic or helper T-cells, their infiltration into the mouse spinal cord has been reported to begin at 14 days post-injury and only reaches significantly elevated levels versus uninjured controls at 42 days post-injury^{188,207}. With the late recruitment of T-cells into the SCI lesion, we theorized that the early benefits seen in the locomotive tests (prior to 14 days in rotarod and horizontal ladder tests) may be due to other GzmB-expressing cells, such as macrophages or microglia. Supporting this, GzmB has been identified in macrophages in human atherosclerotic plaques and in cultured human macrophages¹¹⁶. In our study, GzmB was detected in CD68+ cells which represent either or both macrophages and microglia at 7 days post-injury. Although GzmB appeared to cluster to groups of CD68+ cells, not all CD68+ cells were GzmB+. This suggests that GzmB expression may be dependent on macrophage polarization (M1, M2a, M2b or M2c). M1 macrophages dominate the mouse spinal cord lesion post injury and contribute to neurotoxicity, while M2 macrophages promote an environment of axonal regrowth⁵⁷. Since macrophages have both beneficial and detrimental functions, inhibiting M1 activity or promoting M2 polarization in the lesion shows therapeutic potential in promoting survival and regeneration post injury¹⁹². Kigerl et al. identified

that conditioned medium from M1 macrophages was directly neurotoxic to dorsal root ganglion *in vitro*⁵⁷, suggesting that a secreted factor contributed to this phenotype. It is interesting to speculate that GzmB expression within M1 macrophages contributes to their neurotoxicity.

Finally, to confirm whether the changes in neural cell survival and myelin deposition observed were not due to a decrease in neurotoxic inflammatory mediators we measured the transcript levels of IL-1 β and TNF α by qPCR. While transcript levels were not significantly different between the two groups at 7 days post injury, this may be due to the timepoint investigated. Synthesis and secretion of pro-inflammatory cytokines peaks within 24 hours of the injury before declining to basepoint shortly²⁰⁸. Further studies should identify whether pro-inflammatory cytokines are altered at an early timepoint in GzmB deficient mice.

Chapter 5: Conclusions and Future Directions

In this study, GzmB deficiency in a mouse model of SCI has been shown to be beneficial to locomotor function. This result can be explained by a decrease in immune-cell mediated neural apoptosis and white matter loss, which suggests that GzmB is a neurotoxic protein released during the inflammatory response in SCI. We have identified that GzmB is expressed within macrophages or microglia of a mouse spinal cord lesion, cells that are capable of polarizing towards a neurotoxic phenotype⁵⁷. The work presented here provides a foundation to explore further roles of GzmB in SCI. Specifically, more research needs to investigate whether there is an accumulation of extracellular GzmB in the CSF of patients with acute to chronic SCI. As human samples are rare and difficult to acquire, analyzing CSF of larger mammals first (ie: rats or pigs) may be beneficial to elucidate whether GzmB accumulates extracellularly.

Endogenous extracellular inhibitors for GzmB have shown benefit in mouse models of chronic injuries, including in EAE and aortic aneurysms^{151,175}. As GzmB expression within the spinal cord is localized to cells that do not traditionally express perforin, treatment with an extracellular GzmB inhibitor in SCI may also reduce tissue damage and improve locomotive scores. Further *in vivo* SCI studies should also assess the regenerative capacity of spinal cord tracts. Transgenic mice expressing a mu-crystallin-GFP reporter gene have their CST visualized and can be used to monitor growth of spinal cord tracts across the lesion²⁰⁹. As mentioned in the discussion, remyelination of naked axons after SCI is largely dependent on efficient OPC migration and differentiation to myelinating oligodendrocytes. This response is reduced *in vitro* by cleavage and activation of PAR-1 by extracellular proteases²⁰⁶. As PAR-1 has been implicated in neurotoxicity by extracellular GzmB, future studies should also investigate the role

of GzmB on OPC differentiation and myelination *in vitro*, which may promote remyelination *in vivo*.

The presence of GzmB in subsets of macrophage/microglia suggests differential expression of the protease in these cell types. With the discovery of different polarities of macrophage and microglia in wound responses, it would be beneficial to elucidate which of these express GzmB *in vitro*. Finally, extracellular proteases such as MMPs are secreted by astrocytes, macrophages and neurons which contribute to a breakdown of the BBB. GzmB contributes to vascular barrier breakdown both *in vitro* and *in vivo*¹⁴⁴, however there are different cell types and ECM proteins expressed within the basement membrane of the BBB compared to other vascular beds. Future work in GzmB mediated BBB disruption can be performed both *in vitro* using co-culture systems of brain endothelial cells with astrocytes and pericytes²¹⁰, and *in vivo* using intraperitoneal injections of fluorescent tracers that migrate to the brain and spinal cord²¹¹.

The work presented here builds on the work of others that have shown a neurotoxic role for GzmB in neuroinflammatory conditions^{175,179}. Specific mechanisms of GzmB-mediated pathology are still to be elucidated, and future work should expand the specific macrophage/microglia polarity responsible for secreting GzmB. Most importantly, there may be therapeutic benefit from the inhibition of extracellular GzmB in SCI. A summary of key findings is provided in Figure 10 below.

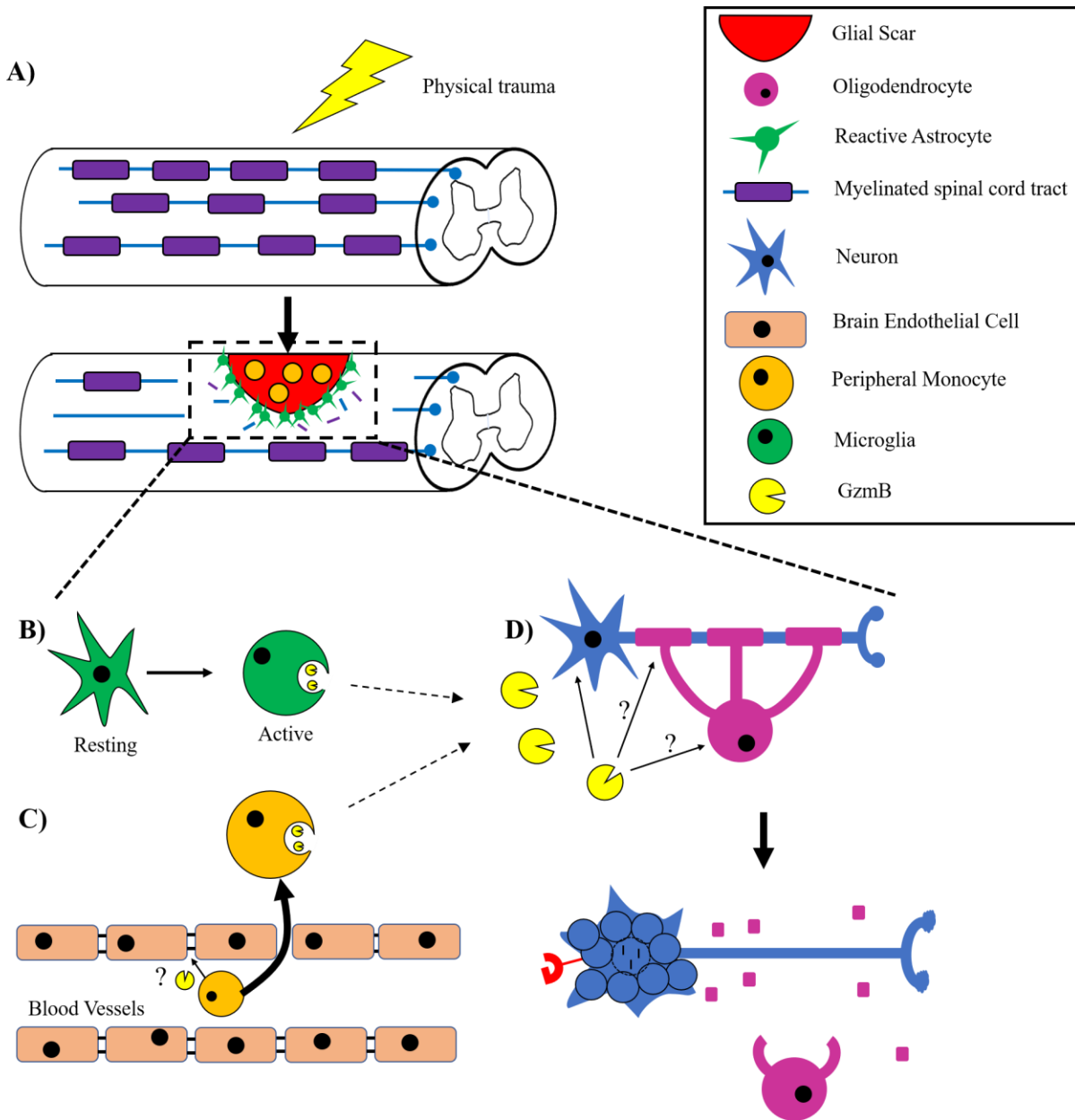


Figure 10 Summary of Findings and Hypothesized Mechanism

A) The body’s response to SCI involves demyelination and axonal death. The inflammatory response includes the activation of resident microglia (**B**) and infiltration of peripheral monocytes (**C**) resulting in GzmB secretion into the lesion site. GzmB results in neuron death and white matter loss that may result from oligodendrocyte death, axonal shearing or myelin protein cleavage (**D**).

Bibliography

1. Norenberg MD, Smith J, Marcillo A. The Pathology of Human Spinal Cord Injury: Defining the Problems. *J Neurotrauma*. 2004;21(4):429-440.
doi:10.1089/089771504323004575.
2. Noonan VK, Fingas M, Farry A, et al. Incidence and prevalence of spinal cord injury in Canada: A national perspective. *Neuroepidemiology*. 2012;38(4):219-226.
doi:10.1159/000336014.
3. Krueger H, Noonan VK, Trenaman LM, Joshi P, Rivers CS. The economic burden of traumatic spinal cord injury in Canada. *Chronic Dis Inj Can*. 2013;33(3):113-122.
4. Hou S, Rabchevsky AG. Autonomic consequences of spinal cord injury. *Compr Physiol*. 2014;4(4):1419-1453. doi:10.1002/cphy.c130045.
5. Krassioukov A, Warburton DE, Teasell R, Eng JJ. A systematic review of the management of autonomic dysreflexia after spinal cord injury. *Spinal Cord Inj Rehabil Evid*. 2010;3.0(3):1-33. [_http://www.scireproject.com/book/export/htm](http://www.scireproject.com/book/export/htm).
doi:10.1016/j.apmr.2008.10.017.A.
6. Allison DJ, Ditor DS. Immune dysfunction and chronic inflammation following spinal cord injury. *Spinal Cord*. 2015;53(1):14-18. doi:10.1038/sc.2014.184.
7. Diaz E, Morales H. Spinal Cord Anatomy and Clinical Syndromes. *Semin Ultrasound, CT MRI*. 2016;37(5):360-371. doi:10.1053/j.sult.2016.05.002.
8. Bican O, Minagar A, Pruitt AA. The Spinal Cord. A Review of Functional Neuroanatomy. *Neurol Clin*. 2013;31(1):1-18. doi:10.1016/j.ncl.2012.09.009.
9. de Girolami U, Bale TA. *Spinal Cord*. Vol 145. 1st ed. Elsevier B.V.; 2017.
doi:10.1016/B978-0-12-802395-2.00029-8.

10. Nielsen JB. Human Spinal Motor Control. *Annu Rev Neurosci.* 2016;39(1):81-101. doi:10.1146/annurev-neuro-070815-013913.
11. Juvin L. Propriospinal Circuitry Underlying Interlimb Coordination in Mammalian Quadrupedal Locomotion. *J Neurosci.* 2005;25(25):6025-6035. doi:10.1523/JNEUROSCI.0696-05.2005.
12. Rahimi J, Woehrer A. *Overview of Cerebrospinal Fluid Cytology.* Vol 145. 1st ed. Elsevier B.V.; 2017. doi:10.1016/B978-0-12-802395-2.00035-3.
13. Sakka L, Coll G, Chazal J. Anatomy and physiology of cerebrospinal fluid. *Eur Ann Otorhinolaryngol Head Neck Dis.* 2011;128(6):309-316. doi:10.1016/j.anorl.2011.03.002.
14. Blood T, Barrier B, Daneman R, Prat A. The Blood –Brain Barrier. 2015:1-23. doi:10.1101/cshperspect.a020412.
15. MacVicar BA, Newman EA. Astrocyte Regulation of Blood Flow in the Brain. *Cold Spring Harb Perspect Biol.* 2015;7:1-15. doi:10.1101/cshpespect.at020388.
16. Baeten KM, Akassoglou K. Extracellular Matrix and Matrix Receptors in Blood-Brain Barrier Formation and Stroke. *Dev Neurobiol.* 2012;71(11):1018-1039. doi:10.1002/dneu.20954.Extracellular.
17. Lakhan SE, Kirchgessner A, Tepper D, Leonard A. Matrix metalloproteinases and blood-brain barrier disruption in acute ischemic stroke. *Front Neurol.* 2013;4 APR(April):1-15. doi:10.3389/fneur.2013.00032.
18. Dietrich JB. The adhesion molecule ICAM-1 and its regulation in relation with the blood-brain barrier. *J Neuroimmunol.* 2002;128(1-2):58-68. doi:10.1016/S0165-5728(02)00114-5.
19. N YG and GD. Cell Adhesion Molecules and Ischemic Stroke. *Neurol Res.*

- 2008;30(8):783-793. doi:10.1179/174313208X341085.CELL.
20. Sharief MK, Noori MA, Ciardi M, Cirelli A, Thompson EJ. Increased levels of circulating ICAM-1 in serum and cerebrospinal fluid of patients with active multiple sclerosis. Correlation with TNF- α and blood-brain barrier damage. *J Neuroimmunol*. 1993;43(1-2):15-21. doi:10.1016/0165-5728(93)90070-F.
 21. Reboldi A, Coisne C, Baumjohann D, et al. C-C chemokine receptor 6 – regulated entry of T H -17 cells into the CNS through the choroid plexus is required for the initiation of EAE. 2009;10(5):514-524. doi:10.1038/ni.1716.
 22. Greenwood J, Heasman SJ, Greenwood J, et al. Review : Leucocyte – endothelial cell crosstalk at the blood – brain barrier : A prerequisite for successful immune cell entry to the brain. 2011:24-39. doi:10.1111/j.1365-2990.2010.01140.x.
 23. Isaac Yang, Seunggu J. Han, Gurvinder Kaur, Courtney Crane and ATP. The Role of Microglia in Central Nervous System Immunity and Glioma Immunology. *J Clin Neurosci*. 2010;17(1):6-10. doi:10.1016/j.jocn.2009.05.006.The.
 24. Rua R, McGavern DB. Advances in Meningeal Immunity. *Trends Mol Med*. 2018;24(6):542-559. doi:10.1016/j.molmed.2018.04.003.
 25. Louveau A, Plog BA, Antila S, Alitalo K, Nedergaard M, Kipnis J. Understanding the functions and relationships of the glymphatic system and meningeal lymphatics. *J Clin Invest*. 2017;127(9):3210-3219. doi:10.1172/JCI90603.
 26. Louveau A, Harris TH, Kipnis J. Revisiting the concept of CNS immune privilege Antoine. *Trends Immunol*. 2015;36(10):569-577. doi:10.1016/j.it.2015.08.006.Revisiting.
 27. Dumont RJ, Okonkwo DO, Verma S, et al. Acute spinal cord injury, part I: pathophysiologic mechanisms. *Clin Neuropharmacol*. 2001;24(5):254-264.

- doi:10.1097/00002826-200109000-00002.
28. Figley SA, Khosravi R, Legasto JM, Tseng Y-F, Fehlings MG. Characterization of Vascular Disruption and Blood–Spinal Cord Barrier Permeability following Traumatic Spinal Cord Injury. *J Neurotrauma*. 2014;31(6):541-552. doi:10.1089/neu.2013.3034.
 29. Oyinbo CA. Secondary injury mechanisms in traumatic spinal cord injury: A nugget of this multiply cascade. *Acta Neurobiol Exp (Wars)*. 2011;71(2):281-299. doi:7128 [pii].
 30. Park E, Velumian AA, Fehlings MG. The Role of Excitotoxicity in Secondary Mechanisms of Spinal Cord Injury: A Review with an Emphasis on the Implications for White Matter Degeneration. *J Neurotrauma*. 2004;21(6):754-774.
doi:10.1089/0897715041269641.
 31. Fernández-Klett F, Priller J. The fibrotic scar in neurological disorders. *Brain Pathol*. 2014;24(4):404-413. doi:10.1111/bpa.12162.
 32. Okada S, Hara M, Kobayakawa K, Matsumoto Y, Nakashima Y. Astrocyte reactivity and astrogliosis after spinal cord injury. *Neurosci Res*. 2018;126:39-43.
doi:10.1016/j.neures.2017.10.004.
 33. Zhang N, Yin Y, Xu S-J, Wu Y-P, Chen W-S. Inflammation & apoptosis in spinal cord injury. *Indian J Med Res*. 2012;135(March):287-296.
<http://www.pubmedcentral.nih.gov/articlerender.fcgi?artid=3361863&tool=pmcentrez&rendertype=abstract>.
 34. Mortazavi MM, Verma K, Harmon OA, et al. The microanatomy of spinal cord injury: A review. *Clin Anat*. 2015;28(1):27-36. doi:10.1002/ca.22432.
 35. Faden AI, Wu J, Stoica BA, Loane DJ. Progressive inflammation-mediated neurodegeneration after traumatic brain or spinal cord injury. *Br J Pharmacol*.

- 2016;173(4):681-691. doi:10.1111/bph.13179.
36. Hausmann ON. Post-traumatic inflammation following spinal cord injury. *Spinal Cord*. 2003;41(7):369-378. doi:10.1038/sj.sc.3101483.
 37. Okada S. The pathophysiological role of acute inflammation after spinal cord injury. *Inflamm Regen*. 2016;36(1):20. doi:10.1186/s41232-016-0026-1.
 38. Whetstone WD, Hsu JC, Eisenberg M, Werb Z, Linda J. Blood-Spinal Cord Barrier After Spinal Cord Injury: Relation to Revascularization and Wound Healing. 2010;74(2):227-239. doi:10.1002/jnr.10759.Blood-Spinal.
 39. Bartanusz V, Jezova D, Alajajian B, Digicaylioglu M. The blood-spinal cord barrier: Morphology and clinical implications. *Ann Neurol*. 2011;70(2):194-206. doi:10.1002/ana.22421.
 40. Liu S, Narayana P a. Blood-Spinal Cord Barrier Permeability in Experimental Spinal Cord Injury: Dynamic Contrast-Enhanced Magnetic Resonance Imaging. 2009;22(3):332-341. doi:10.1002/nbm.1343.Blood-Spinal.
 41. Wells JE, Rice TK, Nuttall RK, et al. An adverse role for matrix metalloproteinase 12 after spinal cord injury in mice. *J Neurosci*. 2003;23(31):10107-10115. doi:23/31/10107 [pii].
 42. Noble LJ, Donovan F, Igarashi T, Goussev S, Werb Z. Matrix Metalloproteinases Limit Functional Recovery after Spinal Cord Injury by Modulation of Early Vascular Events. *J Neurosci*. 2002;22(17):7526–7535. doi:10.1109/TMI.2012.2196707.Separate.
 43. Lee JY, Choi HY, Ahn HJ, Ju BG, Yune TY. Matrix metalloproteinase-3 promotes early blood-spinal cord barrier disruption and hemorrhage and impairs long-term neurological recovery after spinal cord injury. *Am J Pathol*. 2014;184(11):2985-3000.

- doi:10.1016/j.ajpath.2014.07.016.
44. Neirinckx V, Coste C, Franzen R, Gothot A, Rogister B, Wislet S. Neutrophil contribution to spinal cord injury and repair. *J Neuroinflammation*. 2014;11(1):150.
doi:10.1186/s12974-014-0150-2.
 45. Gadani SP, Walsh JT, Lukens JR, Kipnis J. Dealing with Danger in the CNS: The Response of the Immune System to Injury. *Neuron*. 2015;87(1):47-62.
doi:10.1016/j.neuron.2015.05.019.
 46. Nguyen HX, Barr TJO, Anderson AJ. Polymorphonuclear leukocytes promote neurotoxicity through release of matrix metalloproteinases , reactive oxygen species , and TNF- a. 2007:900-912. doi:10.1111/j.1471-4159.2007.04643.x.
 47. Saiwai H, Ohkawa Y, Yamada H, et al. The LTB4-BLT1 axis mediates neutrophil infiltration and secondary injury in experimental spinal cord injury. *Am J Pathol*. 2010;176(5):2352-2366. doi:10.2353/ajpath.2010.090839.
 48. Xiang Zhou, Xijing He YR. Function of microglia and macrophages in secondary damage after SCI. *Neural Regen Res*. 2014;9(20):1787-1795.
 49. Carson MJ, Thrash JC, Walter B. The cellular response in neuroinflammation: The role of leukocytes, microglia and astrocytes in neuronal death and survival. *Clin Neurosci*. 2009;6(5):237-245. doi:10.1016/j.cnr.2006.09.004.The.
 50. David S, Kroner A. Repertoire of microglial and macrophage responses after spinal cord injury. *Nat Rev Neurosci*. 2011;12(7):388-399. doi:10.1038/nrn3053.
 51. David S, Greenhalgh AD, Kroner A. Macrophage and microglial plasticity in the injured spinal cord. *Neuroscience*. 2015;307:311-318. doi:10.1016/j.neuroscience.2015.08.064.
 52. Gensel JC, Zhang B. Macrophage activation and its role in repair and pathology after

- spinal cord injury. *Brain Res.* 2015;1619:1-11. doi:10.1016/j.brainres.2014.12.045.
53. Ferrante CJ, Leibovich SJ. Regulation of Macrophage Polarization and Wound Healing. 2012;1(1):10-16. doi:10.1089/wound.2011.0307.
 54. Zhou Z, Peng X, Insolera R, Fink DJ, Mata M. IL-10 promotes neuronal survival following spinal cord injury. *Exp Neurol.* 2009;220(1):183-190. doi:10.1016/j.expneurol.2009.08.018.IL-10.
 55. Ma SF, Chen YJ, Zhang JX, et al. Adoptive transfer of M2 macrophages promotes locomotor recovery in adult rats after spinal cord injury. *Brain Behav Immun.* 2015;45:157-170. doi:10.1016/j.bbi.2014.11.007.
 56. Francos-Quijorna I, Amo-Aparicio J, Martinez-Muriana A, López-Vales R. IL-4 drives microglia and macrophages toward a phenotype conducive for tissue repair and functional recovery after spinal cord injury. *Glia.* 2016;64(12):2079-2092. doi:10.1002/glia.23041.
 57. Kigerl KA, Gensel JC, Ankeny DP, Alexander JK, Donnelly DJ, Popovich PG. Identification of two distinct macrophage subsets with divergent effects causing either neurotoxicity or regeneration in the injured mouse spinal cord. *J Neurosci.* 2010;29(43):13435-13444. doi:10.1523/JNEUROSCI.3257-09.2009.Identification.
 58. Greenhalgh AD, David S. Differences in the Phagocytic Response of Microglia and Peripheral Macrophages after Spinal Cord Injury and Its Effects on Cell Death. *J Neurosci.* 2014;34(18):6316-6322. doi:10.1523/JNEUROSCI.4912-13.2014.
 59. Hsieh CL, Koike M, Spusta SC, et al. A role for TREM2 ligands in the phagocytosis of apoptotic neuronal cells by microglia. *J Neurochem.* 2009;109(4):1144-1156. doi:10.1111/j.1471-4159.2009.06042.x.
 60. Han D, Yu Z, Liu W, et al. Plasma Hemopexin ameliorates murine spinal cord injury by

- switching microglia from the M1 state to the M2 state. *Cell Death Dis.* 2018;9(2).
doi:10.1038/s41419-017-0236-8.
61. Jones TB. Lymphocytes and autoimmunity after spinal cord injury. *Exp Neurol.* 2014;258:78-90. doi:10.1016/j.expneurol.2014.03.003.
 62. Smith-garvin JE, Koretzky GA, Jordan MS. T Cell Activation Jennifer. *Annu Rev Immunol.* 2010;591-619. doi:10.1146/annurev.immunol.021908.132706.T.
 63. Donnelly DJ, Popovich PG. Inflammation and its role in neuroprotection, axonal regeneration and functional recovery after spinal cord injury. *Exp Neurol.* 2009;209(2):378-388. doi:10.1016/j.expneurol.2007.06.009.Inflammation.
 64. Popovich DPA and PG. Mechanisms and implications of adaptive immune responses after traumatic spinal cord injury. *Neuroscience.* 2010;158(3):1112-1121.
doi:10.1016/j.neuroscience.2008.07.001.Mechanisms.
 65. Zajarías-Fainsod D, Carrillo-Ruiz J, Mestre H, Grijalva I, Madrazo I, Ibarra A. Autoreactivity against myelin basic protein in patients with chronic paraplegia. *Eur Spine J.* 2012;21(5):964-970. doi:10.1007/s00586-011-2060-7.
 66. Jiang H, Braunstein NS, Yu B, Winchester R, Chess L. CD8⁺ T cells control the TH phenotype of MBP-reactive CD4⁺ T cells in EAE mice. 2001;98(11):4-9.
 67. Autoimmune T cells protect neurons from secondary degeneration after central nervous system axotomy. 1999:49-55.
 68. Fisher J, Levkovitch-verbin H, Schori H, et al. Vaccination for Neuroprotection in the Mouse Optic Nerve : Implications for Optic Neuropathies. 2001;21(1):136-142.
 69. Hu JG, Shi LL, Chen YJ, et al. Differential effects of myelin basic protein-activated Th1 and Th2 cells on the local immune microenvironment of injured spinal cord. *Exp Neurol.*

- 2016;277:190-201. doi:10.1016/j.expneurol.2016.01.002.
70. Regulatory_t_cells_exhibit_neuroprotective effect in a mouse model of TBI.PDF.
 71. Kipnis J, Mizrahi T, Hauben E, Shaked I, Shevach E, Schwartz M. Neuroprotective autoimmunity : Naturally occurring CD4⁺ CD25⁺ regulatory T cells suppress the ability to withstand injury to the central nervous system. 2002.
 72. Filiano AJ, Gadani SP, Kipnis J. How and why do T cells and their derived cytokines affect the injured and healthy brain? *Nat Rev Neurosci*. 2017;18(6):375-384. doi:10.1038/nrn.2017.39.
 73. Cheng P, Kuang F, Ju G. Aescin reduces oxidative stress and provides neuroprotection in experimental traumatic spinal cord injury. *Free Radic Biol Med*. 2016;99:405-417. doi:10.1016/j.freeradbiomed.2016.09.002.
 74. Hall ED, Wang JA, Bosken JM, Singh IN. Lipid peroxidation in brain or spinal cord mitochondria after injury. *J Bioenerg Biomembr*. 2016;48(2):169-174. doi:10.1007/s10863-015-9600-5.
 75. Takagi T, Takayasu M, Mizuno M, Yoshimoto M, Yoshida J. Caspase Activation in Neuronal and Glial Apoptosis Following Spinal Cord Injury in Mice. *Neurol Med Chir*. 2003;43:20-30. https://www.jstage.jst.go.jp/article/nmc/43/1/43_1_20/_pdf.
 76. Sobrido-cameán D, Barreiro-iglesias A. Role of Caspase-8 and Fas in Cell Death After Spinal Cord Injury. 2018;11(April):1-9. doi:10.3389/fnmol.2018.00101.
 77. Genovese T, Mazzon E, Crisafulli C, et al. TNF- α blockage in a mouse model of SCI: Evidence for improved outcome. *Shock*. 2008;29(1):32-41. doi:10.1097/shk.0b013e318059053a.
 78. Cantarella G, Di Benedetto G, Scollo M, et al. Neutralization of tumor necrosis factor-

- related apoptosis-inducing ligand reduces spinal cord injury damage in mice. *Neuropsychopharmacology*. 2010;35(6):1302-1314. doi:10.1038/npp.2009.234.
79. Chen K-B, Uchida K, Nakajima H, et al. Tumor Necrosis Factor- α Antagonist Reduces Apoptosis of Neurons and Oligodendroglia in Rat Spinal Cord Injury. *Spine (Phila Pa 1976)*. 2011;36(17):1350-1358. doi:10.1097/BRS.0b013e3181f014ec.
80. Neniskyte U, Vilalta A, Brown GC. Tumour necrosis factor alpha-induced neuronal loss is mediated by microglial phagocytosis. *FEBS Lett*. 2014;588(17):2952-2956. doi:10.1016/j.febslet.2014.05.046.
81. Boato F, Rosenberger K, Nelissen S, et al. Absence of IL-1 β positively affects neurological outcome, lesion development and axonal plasticity after spinal cord injury. *J Neuroinflammation*. 2013;10:1-11. doi:10.1186/1742-2094-10-6.
82. Nesic O, Xu G-Y, McAdoo D, Westlund High K, Hulsebosch C, Perez-Polo R. IL-1 Receptor Antagonist Prevents Apoptosis and Caspase-3 Activation after Spinal Cord Injury. *J Neurotrauma*. 2001;18(9):947-956. doi:10.1089/089771501750451857.
83. Renault-Mihara F, Mukaino M, Shinozaki M, et al. Regulation of RhoA by STAT3 coordinates glial scar formation. *J Cell Biol*. 2017;216(8):2533-2550. doi:10.1083/jcb.201610102.
84. Herrmann JE, Imura T, Song B, et al. STAT3 is a Critical Regulator of Astrogliosis and Scar Formation after Spinal Cord Injury. *J Neurosci*. 2008;28(28):7231-7243. doi:10.1523/JNEUROSCI.1709-08.2008.
85. Bradbury EJ, Moon LDF, Popat RJ, et al. Chondroitinase ABC promotes functional recovery after spinal cord injury. *Nature*. 2002;416(6881):636-640. doi:10.1038/416636a.
86. Anderson MA, Burda JE, Ren Y, et al. Astrocyte scar formation AIDS central nervous

- system axon regeneration. *Nature*. 2016;532(7598):195-200. doi:10.1038/nature17623.
87. Faulkner JR. Reactive Astrocytes Protect Tissue and Preserve Function after Spinal Cord Injury. *J Neurosci*. 2004;24(9):2143-2155. doi:10.1523/JNEUROSCI.3547-03.2004.
88. Liddelow SA, Guttenplan KA, Clarke LE, et al. Neurotoxic reactive astrocytes are induced by activated microglia. *Nature*. 2017;541(7638):481-487. doi:10.1038/nature21029.
89. Soderblom C, Luo X, Blumenthal E, et al. Perivascular Fibroblasts Form the Fibrotic Scar after Contusive Spinal Cord Injury. *J Neurosci*. 2013;33(34):13882-13887. doi:10.1523/JNEUROSCI.2524-13.2013.
90. Dias DO, Kim H, Holl D, et al. Reducing Pericyte-Derived Scarring Promotes Recovery after Spinal Cord Injury. *Cell*. 2018;173(1):153-165.e22. doi:10.1016/j.cell.2018.02.004.
91. Shearer MC, Fawcett JW. The astrocyte/meningeal cell interface--a barrier to successful nerve regeneration? *Cell Tissue Res*. 2001;305(2):267-273.
92. Voskoboinik I, Whisstock JC, Trapani JA. Perforin and granzymes: Function, dysfunction and human pathology. *Nat Rev Immunol*. 2015;15(6):388-400. doi:10.1038/nri3839.
93. Manuscript A, Death C. Death by a Thousand Cuts: Granzyme Pathways of Programmed Cell Death. 2009:389-420. doi:10.1146/annurev.immunol.26.021607.090404.Death.
94. Joeckel LT, Bird PI. Are all granzymes cytotoxic in vivo? *Biol Chem*. 2014;395(2):181-202. doi:10.1515/hsz-2013-0238.
95. Boivin WA, Cooper DM, Hiebert PR, Granville DJ. Intracellular versus extracellular granzyme B in immunity and disease: Challenging the dogma. *Lab Investig*. 2009;89(11):1195-1220. doi:10.1038/labinvest.2009.91.
96. Edwards KM, Kam CM, Powers JC, Trapani JA. The human cytotoxic T cell granule

- serine protease granzyme H has chymotrypsin-like (chymase) activity and is taken up into cytoplasmic vesicles reminiscent of granzyme B-containing endosomes. *J Biol Chem.* 1999;274(43):30468-30473. doi:10.1074/jbc.274.43.30468.
97. Ewen CL, Kane KP, Bleackley RC. A quarter century of granzymes. *Cell Death Differ.* 2012;19(1):28-35. doi:10.1038/cdd.2011.153.
98. Heusel JW, Wesselschmidt RL, Russell JH, Ley TJ. Cytotoxic Lymphocytes Require Granzyme B for the Rapid Induction of DNA Fragmentation and Apoptosis in Allogeneic Target Cells. 1994;76(1980).
99. Fellows E, Gil-Parrado S, Jenne DE, Kurschus FC. Natural killer cell-derived human granzyme H induces an alternative, caspase-independent cell-death program. *Blood.* 2007;110(2):544-552. doi:10.1182/blood-2006-10-051649.
100. Martinvalet D, Zhu P, Lieberman J. Granzyme A Induces Caspase-Independent Mitochondrial Damage , a Required First Step for Apoptosis. 2005;22:355-370. doi:10.1016/j.immuni.2005.02.004.
101. Hink-schauer C, Estébanez-perpiñá E, Kurschus FC, Bode W, Jenne DE. Crystal structure of the apoptosis-inducing human granzyme A dimer. 2003;10(7).
102. Metkar SS, Mena C, Pardo J, et al. Human and Mouse Granzyme A Induce a Proinflammatory Cytokine Response. *Immunity.* 2008;29(5):720-733. doi:10.1016/j.immuni.2008.08.014.
103. Anthony DA, Andrews DM, Watt S V., Trapani JA, Smyth MJ. Functional dissection of the granzyme family: Cell death and inflammation. *Immunol Rev.* 2010;235(1):73-92. doi:10.1111/j.0105-2896.2010.00907.x.
104. Rucevic M, Fast LD, Jay GD, et al. ALTERED LEVELS AND MOLECULAR FORMS

- OF GRANZYME K IN PLASMA FROM SEPTIC PATIENTS Sepsis is a consequence of a dysregulated systemic. 2007;27(5):488-493. doi:10.1097/01.shk.0000246905.24895.e5.
105. Bratke K, Klug A, Julius P, et al. Granzyme K : a novel mediator in acute airway inflammation. doi:10.1136/thx.2007.091215.
 106. Wensink AC, Kemp V, Fermie J, et al. Granzyme K synergistically potentiates LPS-induced cytokine responses in human monocytes. *Proc Natl Acad Sci.* 2014;111(16):5974-5979. doi:10.1073/pnas.1317347111.
 107. Cooper DM, Petchkovsky D V., Hackett TL, Knight DA, Granville DJ. Granzyme K activates protease-activated receptor-1. *PLoS One.* 2011;6(6):1-9. doi:10.1371/journal.pone.0021484.
 108. Sharma M, Merkulova Y, Raithatha S, et al. Extracellular granzyme K mediates endothelial activation through the cleavage of protease-activated receptor-1. *FEBS J.* 2016;283(9):1734-1747. doi:10.1111/febs.13699.
 109. Griffiths GM, Isaaz S. Granzymes A and B are targeted to the lytic granules of lymphocytes by the mannose-6-phosphate receptor. *J Cell Biol.* 1993;120(4):885-896. doi:10.1083/jcb.120.4.885.
 110. Kurschus FC, Kleinschmidt M, Fellows E, et al. Killing of target cells by redirected granzyme B in the absence of perforin. *FEBS Lett.* 2004;562(1-3):87-92. doi:10.1016/S0014-5793(04)00187-5.
 111. D'Angelo ME, Bird PI, Peters C, Reinheckel T, Trapaniand JA, Sutton VR. Cathepsin H is an additional convertase of pro-granzyme B. *J Biol Chem.* 2010;285(27):20514-20519. doi:10.1074/jbc.M109.094573.
 112. Balaji KN, Schaschke N, Machleidt W, Catalfamo M, Henkart PA. Surface Cathepsin B

- Protects Cytotoxic Lymphocytes from Self-destruction after Degranulation. *J Exp Med*. 2002;196(4):493-503. doi:10.1084/jem.20011836.
113. Bratke K, Kuepper M, Bade B, Virchow JC, Luttmann W. Differential expression of human granzymes A, B, and K in natural killer cells and during CD8+ T cell differentiation in peripheral blood. *Eur J Immunol*. 2005;35(9):2608-2616. doi:10.1002/eji.200526122.
114. Lin L, Couturier J, Yu X, Medina MA, Kozinetz CA, Lewis DE. Granzyme B secretion by human memory CD4 T cells is less strictly regulated compared to memory CD8 T cells. 2014;15(1):1-15. doi:10.1186/s12865-014-0036-1.
115. Janas ML, Groves P, Kienzle N, Kelso A. IL-2 Regulates Perforin and Granzyme Gene Expression in CD8+ T Cells Independently of Its Effects on Survival and Proliferation. *J Immunol*. 2005;175(12):8003-8010. doi:10.4049/jimmunol.175.12.8003.
116. Kim WJ, Kim H, Suk K, Lee WH. Macrophages express granzyme B in the lesion areas of atherosclerosis and rheumatoid arthritis. *Immunol Lett*. 2007;111(1):57-65. doi:10.1016/j.imlet.2007.05.004.
117. Intracellular versus extracellular granzyme B in immunity and disease: challenging the dogma.
118. Chávez-Galán L, Arenas-Del Angel MC, Zenteno E, Chávez R, Lascurain R. Cell death mechanisms induced by cytotoxic lymphocytes. *Cell Mol Immunol*. 2009;6(1):15-25. doi:10.1038/cmi.2009.3.
119. Afonina IS, Cullen SP, Martin SJ. Cytotoxic and non-cytotoxic roles of the CTL/NK protease granzyme B. *Immunol Rev*. 2010;235(1):105-116. doi:10.1111/j.0105-2896.2010.00908.x.

120. Metkar SS, Wang B, Aguilar-Santelises M, et al. Cytotoxic cell granule-mediated apoptosis: Perforin delivers granzyme b-serglycin complexes into target cells without plasma membrane pore formation. *Immunity*. 2002;16(3):417-428. doi:10.1016/S1074-7613(02)00286-8.
121. Cullen SP, Martin SJ. Mechanisms of granule-dependent killing. *Cell Death Differ*. 2008;15(2):251-262. doi:10.1038/sj.cdd.4402244.
122. Kupfer A, Dennertt G, Singer SJ. Polarization of the Golgi apparatus and the microtubule-organizing center within cloned natural killer cells bound to their targets *Cell Biology* : 1983;80(December):7224-7228.
123. Hoves S, Trapani JA, Voskoboinik I. The battlefield of perforin/granzyme cell death pathways. *J Leukoc Biol*. 2010;87(2):237-243. doi:10.1189/jlb.0909608.
124. Voskoboinik I, Smyth MJ, Trapani JA. Perforin-mediated target-cell death and immune homeostasis. *Nat Rev Immunol*. 2006;6(12):940-952. doi:10.1038/nri1983.
125. Hengartner MO. The biochemistry of apoptosis. *Nat Insight*. 2000;407(15):770-776. doi:10.1074/jbc.R100062200.
126. Adrain C, Murphy BM, Martin SJ. Molecular ordering of the caspase activation cascade initiated by the cytotoxic T lymphocyte/natural killer (CTL/NK) protease granzyme B. *J Biol Chem*. 2005;280(6):4663-4673. doi:10.1074/jbc.M410915200.
127. Susanto O, Trapani J a., Brasacchio D. Controversies in granzyme biology. *Tissue Antigens*. 2012;80(6):477-487. doi:10.1111/tan.12014.
128. Granzyme B in Injury, Inflammation and Repair.
129. Tschopp CM, Spiegl N, Didichenko S, et al. Granzyme B , a novel mediator of allergic inflammation : its induction and release in blood basophils and human asthma Granzyme

- B , a novel mediator of allergic inflammation : its induction and release in blood basophils and human asthma. 2012;108(7):2290-2299. doi:10.1182/blood-2006-03-010348.
130. Buzza MS, Bird PI. Extracellular granzymes: Current perspectives. *Biol Chem.* 2006;387(7):827-837. doi:10.1515/BC.2006.106.
 131. Malmeström C, Lycke J, Haghighi S, et al. Relapses in multiple sclerosis are associated with increased CD8+T-cell mediated cytotoxicity in CSF. *J Neuroimmunol.* 2008;196(1-2):159-165. doi:10.1016/j.jneuroim.2008.03.001.
 132. Bratke K, Böttcher B, Leeder K, et al. Increase in granzyme B+lymphocytes and soluble granzyme B in bronchoalveolar lavage of allergen challenged patients with atopic asthma. *Clin Exp Immunol.* 2004;136(3):542-548. doi:10.1111/j.1365-2249.2004.02468.x.
 133. Soriano C, Mukaro V, Hodge G, et al. Increased proteinase inhibitor-9 (PI-9) and reduced granzyme B in lung cancer: mechanism for immune evasion? *Lung cancer.* 2012;77(1):38-45. doi:10.1016/j.lungcan.2012.01.017.
 134. Prakash MD, Bird CH, Bird PI. Active and zymogen forms of granzyme B are constitutively released from cytotoxic lymphocytes in the absence of target cell engagement. *Immunol Cell Biol.* 2009;87(3):249-254. doi:10.1038/icb.2008.98.
 135. Buzza MS, Zamurs L, Sun J, et al. Extracellular matrix remodeling by human granzyme B via cleavage of vitronectin, fibronectin, and laminin. *J Biol Chem.* 2005;280(25):23549-23558. doi:10.1074/jbc.M412001200.
 136. Hiebert PR, Wu D, Granville DJ. Granzyme B degrades extracellular matrix and contributes to delayed wound closure in apolipoprotein e knockout mice. *Cell Death Differ.* 2013;20(10):1404-1414. doi:10.1038/cdd.2013.96.
 137. Russo V, Klein T, Lim DJ, et al. Granzyme B is elevated in autoimmune blistering

- diseases and cleaves key anchoring proteins of the dermal-epidermal junction. *Sci Rep.* 2018;(June):1-11. doi:10.1038/s41598-018-28070-0.
138. Maquart FX, Monboisse JC. Extracellular matrix and wound healing. *Pathol Biol.* 2014;62(2):91-95. doi:10.1016/j.patbio.2014.02.007.
139. Breitzkreutz D, Koxholt I, Thiemann K, Nischt R. Skin basement membrane: The foundation of epidermal integrity - BM functions and diverse roles of bridging molecules nidogen and perlecan. *Biomed Res Int.* 2013;2013. doi:10.1155/2013/179784.
140. Turner CT, Lim D, Granville DJ. Granzyme B in skin inflammation and disease. *Matrix Biol.* 2017;1-15. doi:10.1016/j.matbio.2017.12.005.
141. Choy JC, Hung VHY, Hunter AL, et al. Granzyme B induces smooth muscle cell apoptosis in the absence of perforin: Involvement of extracellular matrix degradation. *Arterioscler Thromb Vasc Biol.* 2004;24(12):2245-2250. doi:10.1161/01.ATV.0000147162.51930.b7.
142. Afonina IS, Tynan GA, Logue SE, et al. Granzyme B-dependent proteolysis acts as a switch to enhance the proinflammatory activity of IL-1 α . *Mol Cell.* 2011;44(2):265-278. doi:10.1016/j.molcel.2011.07.037.
143. Omoto Y, Yamanaka K, Tokime K, et al. Granzyme B is a novel interleukin-18 converting enzyme. *J Dermatol Sci.* 2010;59(2):129-135. doi:10.1016/j.jdermsci.2010.05.004.
144. Shen Y, Cheng F, Sharma M, et al. Granzyme B Deficiency Protects against Angiotensin II-Induced Cardiac Fibrosis. *Am J Pathol.* 2016;186(1):87-100. doi:10.1016/j.ajpath.2015.09.010.
145. Prakash MD, Munoz MA, Jain R, et al. Granzyme B promotes cytotoxic lymphocyte

- transmigration via basement membrane remodeling. *Immunity*. 2014;41(6):960-972.
doi:10.1016/j.immuni.2014.11.012.
146. Hendel A, Hsu I, Granville DJ. Granzyme B releases vascular endothelial growth factor from extracellular matrix and induces vascular permeability. *Lab Invest*. 2014;94(7):716-725. doi:10.1038/labinvest.2014.62.
147. Taylor AW. Review of the activation of TGF- in immunity. *J Leukoc Biol*. 2008;85(1):29-33. doi:10.1189/jlb.0708415.
148. Akhurst RJ. TGF β signaling in health and disease. *Nat Genet*. 2004;36(8):790-792. doi:10.1038/ng0804-790.
149. Boivin WA, Shackelford M, Vanden Hoek A, et al. Granzyme B cleaves decorin, biglycan and soluble betaglycan, releasing active transforming growth factor- β 1. *PLoS One*. 2012;7(3):1-8. doi:10.1371/journal.pone.0033163.
150. Chamberlain CM, Ang LS, Boivin WA, et al. Perforin-independent extracellular granzyme B activity contributes to abdominal aortic aneurysm. *Am J Pathol*. 2010;176(2):1038-1049. doi:10.2353/ajpath.2010.090700.
151. Ang LS, Boivin WA, Williams SJ, et al. Serpina3n attenuates granzyme B-mediated decorin cleavage and rupture in a murine model of aortic aneurysm. *Cell Death Dis*. 2011;2(9):e209-10. doi:10.1038/cddis.2011.88.
152. Hiebert PR, Boivin WA, Abraham T, Pazooki S, Zhao H, Granville DJ. Granzyme B contributes to extracellular matrix remodeling and skin aging in apolipoprotein E knockout mice. *Exp Gerontol*. 2011;46(6):489-499. doi:10.1016/j.exger.2011.02.004.
153. Shen Y, Zeglinski MR, Turner CT, et al. Topical small molecule granzyme B inhibitor improves remodeling in a murine model of impaired burn wound healing. *Exp Mol Med*.

2018. doi:10.1038/s12276-018-0095-0.
154. Parkinson LG, Toro A, Zhao H, Brown K, Tebbutt SJ, Granville DJ. Granzyme B mediates both direct and indirect cleavage of extracellular matrix in skin after chronic low-dose ultraviolet light irradiation. *Aging Cell*. 2015;14(1):67-77. doi:10.1111/accel.12298.
155. Hernandez-Pigeon H, Jean C, Charruyer A, et al. UVA induces granzyme B in human keratinocytes through MIF: Implication in extracellular matrix remodeling. *J Biol Chem*. 2007;282(11):8157-8164. doi:10.1074/jbc.M607436200.
156. Blanco P, Pitard V, Viallard JF, Taupin JL, Pellegrin JL, Moreau JF. Increase in activated CD8+ T lymphocytes expressing perforin and granzyme B correlates with disease activity in patients with systemic lupus erythematosus. *Arthritis Rheum*. 2005;52(1):201-211. doi:10.1002/art.20745.
157. Lanzavecchia A. How Can Cryptic Epitopes Trigger Autoimmunity? *J Exp Med*. 1995;181(June):1945-1948. doi:10.1084/jem.181.6.1945.
158. Lee PR, Johnson TP, Gnanapavan S, et al. Protease-activated receptor-1 activation by granzyme B causes neurotoxicity that is augmented by interleukin-1 β . *J Neuroinflammation*. 2017;14(1):1-18. doi:10.1186/s12974-017-0901-y.
159. Huang WJ, Chen WW, Zhang X. Multiple sclerosis: Pathology, diagnosis and treatments (review). *Exp Ther Med*. 2017;13(6):3163-3166. doi:10.3892/etm.2017.4410.
160. Giuliani F, Goodyer CG, Antel JP, Yong VW. Vulnerability of Human Neurons to T Cell-Mediated Cytotoxicity. *J Immunol*. 2003;171(1):368-379. doi:10.4049/jimmunol.171.1.368.
161. Jurewicz a, Biddison WE, Antel JP. MHC class I-restricted lysis of human

- oligodendrocytes by myelin basic protein peptide-specific CD8 T lymphocytes. *J Immunol.* 1998;160(6):3056-3059. <http://www.ncbi.nlm.nih.gov/pubmed/9510211>.
162. Haile Y, Simmen KC, Pasichnyk D, et al. Granule-Derived Granzyme B Mediates the Vulnerability of Human Neurons to T Cell-Induced Neurotoxicity. *J Immunol.* 2011;187(9):4861-4872. doi:10.4049/jimmunol.1100943.
163. Puentes F, van der Star BJ, Victor M, et al. Characterization of immune response to neurofilament light in experimental autoimmune encephalomyelitis. *J Neuroinflammation.* 2013;10(1):1. doi:10.1186/1742-2094-10-118.
164. Broux B, Mizze MR, Vanheusden M, et al. IL-15 Amplifies the Pathogenic Properties of CD4⁺ CD28⁻ T Cells in Multiple Sclerosis. *J Immunol.* 2015;194(5):2099-2109. doi:10.4049/jimmunol.1401547.
165. Takeuchi A, Saito T. CD4 CTL, a cytotoxic subset of CD4⁺T cells, their differentiation and function. *Front Immunol.* 2017;8(FEB):1-7. doi:10.3389/fimmu.2017.00194.
166. Raveney BJE, Oki S, Hohjoh H, et al. Eomesodermin-expressing T-helper cells are essential for chronic neuroinflammation. *Nat Commun.* 2015;6:1-11. doi:10.1038/ncomms9437.
167. Wang T, Lee MH, Johnson T, et al. Activated T-Cells Inhibit Neurogenesis by Releasing Granzyme B: Rescue by Kv1.3 Blockers. *J Neurosci.* 2010;30(14):5020-5027. doi:10.1523/JNEUROSCI.0311-10.2010.
168. Neumann H, Medana IM, Bauer J, Lassmann H. Cytotoxic T lymphocytes in autoimmune and degenerative CNS diseases. *Trends Neurosci.* 2002;25(6):313-319. doi:10.1016/S0166-2236(02)02154-9.
169. Mirshafiey A, Kianiaslani M. Autoantigens and autoantibodies in multiple sclerosis. *Iran*

- J Allergy, Asthma Immunol.* 2013;12(4):292-303.
170. Rosen A, Martinvalet D, Lieberman J, Perl A. Cleavage of Transaldolase by Granzyme B Causes the Loss of Enzymatic Activity with Retention of Antigenicity for Multiple Sclerosis Patients. 2011;184(7):4025-4032. doi:10.4049/jimmunol.0804174.Cleavage.
171. Agrawal SM, Silva C, Wang J, Tong JP, Yong VW. A novel anti-EMMPRIN function-blocking antibody reduces T cell proliferation and neurotoxicity: Relevance to multiple sclerosis. *J Neuroinflammation.* 2012;9:1-14. doi:10.1186/1742-2094-9-64.
172. Wang T, Lee MH, Choi E, et al. Granzyme B-Induced Neurotoxicity Is Mediated via Activation of PAR-1 Receptor and Kv1.3 Channel. *PLoS One.* 2012;7(8). doi:10.1371/journal.pone.0043950.
173. Venken K, Hellings N, Liblau R, Stinissen P. Disturbed regulatory T cell homeostasis in multiple sclerosis. *Trends Mol Med.* 2010;16(2):58-68. doi:10.1016/j.molmed.2009.12.003.
174. Bhela S, Kempell C, Manohar M, et al. Non-apoptotic and extracellular activity of Granzyme B mediates resistance to Treg suppression by HLA-DRneg CD25hi CD127lo Tregs in multiple sclerosis and in response to IL-6. *J Immunol.* 2015;194(4):2180-2189. doi:10.4049/jimmunol.1303257.
175. Haile Y, Carmine-Simmen K, Olechowski C, Kerr B, Bleackley RC, Giuliani F. Granzyme B-inhibitor serpin3n induces neuroprotection in vitro and in vivo. *J Neuroinflammation.* 2015;12(1):1-10. doi:10.1186/s12974-015-0376-7.
176. Lewis CA, Manning J, Rossi F, Krieger C. The neuroinflammatory response in ALS: The roles of microglia and T cells. *Neurol Res Int.* 2012;2012. doi:10.1155/2012/803701.
177. Malaspina A, Puentes F, Amor S. Disease origin and progression in amyotrophic lateral

- sclerosis: An immunology perspective. *Int Immunol*. 2015;27(3):117-129.
doi:10.1093/intimm/dxu099.
178. Ilžecka J. Granzymes A and B levels in serum of patients with amyotrophic lateral sclerosis. *Clin Biochem*. 2011;44(8-9):650-653. doi:10.1016/j.clinbiochem.2011.02.006.
179. Chaitanya GV, Kolli M, Babu PP. Granzyme-b mediated cell death in the spinal cord-injured rat model. *Neuropathology*. 2009;29(3):270-279. doi:10.1111/j.1440-1789.2008.00980.x.
180. Haque A, Best SE, Unosson K, et al. Granzyme B Expression by CD8+ T Cells Is Required for the Development of Experimental Cerebral Malaria. *J Immunol*. 2011;186(11):6148-6156. doi:10.4049/jimmunol.1003955.
181. Basso DM, Fisher LC, Anderson AJ, Jakeman LYNB, Tigue DMMC, Popovich PG. Basso Mouse Scale for Locomotion Detects Differences in Recovery after Spinal Cord Injury in Five Common Mouse Strains. 2006;23(5):635-659.
182. Bhalala OG, Pan L, North H, Mcguire T, Kessler JA. Generation of Mouse Spinal Cord Injury Materials and Reagents. 2016;3(17).
<https://www.ncbi.nlm.nih.gov/pmc/articles/PMC4978511/pdf/nihms770745.pdf>.
183. Shiotsuki H, Yoshimi K, Shimo Y, Funayama M, Takamatsu Y. A rotarod test for evaluation of motor skill learning. *J Neurosci Methods*. 2010;189(2):180-185.
doi:10.1016/j.jneumeth.2010.03.026.
184. Manuscript A, Blood W, Count C. Extracellular matrix regulation of inflammation in the healthy and injured spinal cord. 2009;49(18):1841-1850.
doi:10.1016/j.jacc.2007.01.076.White.
185. Cummings BJ, Engesser-cesar C, Anderson AJ. Adaptation of a ladder beam walking task

- to assess locomotor recovery in mice following spinal cord injury. 2008;177(2):232-241.
186. Jakeman LB, Guan Z, Wei P, et al. Traumatic spinal cord injury produced by controlled contusion in mouse. *J Neurotrauma*. 2000;17(4):299-319. doi:10.1089/neu.2000.17.299.
 187. Zhang N, Fang M, Chen H, Gou F, Ding M. Evaluation of spinal cord injury animal models. *Neural Regen Res*. 2014;9(22):2008-2012. doi:10.4103/1673-5374.143436.
 188. Sroga JM, Jones TB, Kigerl KA, McGaughy VM, Popovich PG. Rats and mice exhibit distinct inflammatory reactions after spinal cord injury. *J Comp Neurol*. 2003;462(2):223-240. doi:10.1002/cne.10736.
 189. Li H, Kong W, Chambers CR, et al. The non-psychoactive phytocannabinoid cannabidiol (CBD) attenuates pro-inflammatory mediators, T cell infiltration, and thermal sensitivity following spinal cord injury in mice. *Cell Immunol*. 2018;329(March):1-9. doi:10.1016/j.cellimm.2018.02.016.
 190. Pomeschchik Y, Kidin I, Korhonen P, et al. Interleukin-33 treatment reduces secondary injury and improves functional recovery after contusion spinal cord injury. *Brain Behav Immun*. 2015;44:68-81. doi:10.1016/j.bbi.2014.08.002.
 191. Carelli S, Giallongo T, Gerace C, et al. Neural Stem Cell Transplantation in Experimental Contusive Model of Spinal Cord Injury. *J Vis Exp*. 2014;(94):1-8. doi:10.3791/52141.
 192. Arima H, Hanada M, Hayasaka T, et al. Blockade of IL-6 signaling by MR16-1 inhibits reduction of docosahexaenoic acid-containing phosphatidylcholine levels in a mouse model of spinal cord injury. *Neuroscience*. 2014;269:1-10. doi:10.1016/j.neuroscience.2014.03.012.
 193. Norimatsu Y, Ohmori T, Kimura A, et al. FTY720 improves functional recovery after spinal cord injury by primarily nonimmunomodulatory mechanisms. *Am J Pathol*.

- 2012;180(4):1625-1635. doi:10.1016/j.ajpath.2011.12.012.
194. Coll-Miró M, Francos-Quijorna I, Santos-Nogueira E, et al. Beneficial effects of IL-37 after spinal cord injury in mice. *Proc Natl Acad Sci*. 2016;113(5):1411-1416. doi:10.1073/pnas.1523212113.
195. FENGSHAN YU, HIROSHI KAMADA, KUNIYASU NIIZUMA, HIDENORI ENDO and PHC. Induction of MMP-9 Expression and Endothelial Injury by Oxidative Stress after Spinal Cord Injury. *J Neurotrauma*. 2009;19(3):389-399. doi:10.1016/j.asieco.2008.09.006.EAST.
196. Duan H-Q, Wu Q-L, Yao X, et al. Nafamostat mesilate attenuates inflammation and apoptosis and promotes locomotor recovery after spinal cord injury. *CNS Neurosci Ther*. 2018;(December 2017):1-10. doi:10.1111/cns.12801.
197. Festoff BW, Ameenuddin S, Arnold PM, Wong A, Santacruz KS, Citron BA. Minocycline neuroprotects , reduces microgliosis , and inhibits caspase protease expression early after spinal cord injury. 2006:1314-1326. doi:10.1111/j.1471-4159.2006.03799.x.
198. Jin Y, Yang S, Zhang X. Reduction of neuronal damage and promotion of locomotor recovery after spinal cord injury by early administration of methylprednisolone: possible involvement of autophagy pathway. *RSC Adv*. 2017;7(5):2979-2991. doi:10.1039/c6ra25794a.
199. Xu GY, Hughes MG, Ye Z, Hulsebosch CE, McAdoo DJ. Concentrations of glutamate released following spinal cord injury kill oligodendrocytes in the spinal cord. *Exp Neurol*. 2004;187(2):329-336. doi:10.1016/j.expneurol.2004.01.029.
200. Takahashi JL, Giuliani F, Power C, Imai Y, Yong VW. Interleukin-1 β promotes oligodendrocyte death through glutamate excitotoxicity. *Ann Neurol*. 2003;53(5):588-595.

doi:10.1002/ana.10519.

201. Juliet PAR, Frost EE, Balasubramaniam J, Del Bigio MR. Toxic effect of blood components on perinatal rat subventricular zone cells and oligodendrocyte precursor cell proliferation, differentiation and migration in culture. *J Neurochem.* 2009;109(5):1285-1299. doi:10.1111/j.1471-4159.2009.06060.x.
202. Jones TB, Basso DM, Sodhi A, et al. Pathological CNS autoimmune disease triggered by traumatic spinal cord injury: implications for autoimmune vaccine therapy. *J Neurosci.* 2002;22(7):2690-2700. doi:20026267.
203. Göbel K, Melzer N, Herrmann AM, et al. Collateral neuronal apoptosis in CNS gray matter during an oligodendrocyte-directed CD8+ T Cell Attack. *Glia.* 2010;58(4):469-480. doi:10.1002/glia.20938.
204. Grégoire C-A, Goldenstein BL, Floriddia EM, Barnabé-Heider F, Fernandes KJL. Endogenous neural stem cell responses to stroke and spinal cord injury. *Glia.* 2015;63(8):1469-1482. doi:10.1002/glia.22851.
205. Kotter MR. Myelin Impairs CNS Remyelination by Inhibiting Oligodendrocyte Precursor Cell Differentiation. *J Neurosci.* 2006;26(1):328-332. doi:10.1523/JNEUROSCI.2615-05.2006.
206. Joshua E. Burda, Maja Radulovic, Hyesook Yoon and IAS. Critical Role for PAR1 in Kallikrein 6-Mediated Oligodendroglipathy. *Glia.* 2013;61(9):1456-1470. doi:10.1016/j.asieco.2008.09.006.EAST.
207. Jones TB, Hart RP, Popovich PG. Molecular control of physiological and pathological T-cell recruitment after mouse spinal cord injury. *J Neurosci.* 2005;25(28):6576-6583. doi:10.1523/JNEUROSCI.0305-05.2005.

208. Bartholdi D, Schwab ME. Expression of pro-inflammatory cytokine and chemokine mRNA upon experimental spinal cord injury in mouse: an in situ hybridization study. *Eur J Neurosci.* 1997;9(7):1422-1438.
http://www.ncbi.nlm.nih.gov/entrez/query.fcgi?cmd=Retrieve&db=PubMed&dopt=Citation&list_uids=9240400.
209. Fink KL, Strittmatter SM, Cafferty WBJ. Comprehensive Corticospinal Labeling with mu-crystallin Transgene Reveals Axon Regeneration after Spinal Cord Trauma in *ngr1*^{-/-} Mice. *J Neurosci.* 2015;35(46):15403-15418. doi:10.1523/JNEUROSCI.3165-15.2015.
210. Wilhelm I, Fazakas C, Krizbai IA. In vitro models of the blood-brain barrier. *Acta Neurobiol Exp (Wars).* 2011;71(1):113-128. doi:10.1007/978-1-4939-0320-7_34.
211. Devraj K, Guerit S, Macas J, Reiss Y. An In Vivo Blood-brain Barrier Permeability Assay in Mice Using Fluorescently Labeled Tracers. *J Vis Exp.* 2018;(132). doi:10.3791/57038.